

Modulation of abscisic acid signaling via endosomal TOL proteins

Jeanette Moulinier-Anzola¹ , Maximilian Schwihla¹ , Rebecca Lugsteiner¹, Nils Leibrock¹ ,
Mugurel I. Feraru^{1,2} , Irma Tkachenko¹, Christian Luschign¹ , Elsa Arcalis¹ , Elena Feraru¹ ,
Jorge Lozano-Juste³  and Barbara Korbei¹ 

¹Department of Applied Genetics and Cell Biology, Institute of Molecular Plant Biology, BOKU University, Muthgasse 18, 1190, Vienna, Austria; ²“Gheorghe Rosca Codreanu” National College, Nicolae Balcescu, Barlad, 731183, Vaslui, Romania; ³Instituto de Biología Molecular y Celular de Plantas, Universitat Politècnica de València, Consejo Superior de Investigaciones Científicas, 46022, Valencia, Spain

Summary

Author for correspondence:
Barbara Korbei
Email: barbara.korbei@boku.ac.at

Received: 6 February 2024
Accepted: 25 May 2024

New Phytologist (2024) 243: 1065–1081
doi: 10.1111/nph.19904

Key words: ABA receptors, ABA signaling pathway, ABA transporters, ESCRT, TOL, vacuolar degradation.

- The phytohormone abscisic acid (ABA) functions in the control of plant stress responses, particularly in drought stress. A significant mechanism in attenuating and terminating ABA signals involves regulated protein turnover, with certain ABA receptors, despite their main presence in the cytosol and nucleus, subjected to vacuolar degradation via the Endosomal Sorting Complex Required for Transport (ESCRT) machinery.
- Collectively our findings show that discrete TOM1-LIKE (TOL) proteins, which are functional ESCRT-0 complex substitutes in plants, affect the trafficking for degradation of core components of the ABA signaling and transport machinery.
- *TOL2,3,5* and *6* modulate ABA signaling where they function additively in degradation of ubiquitinated ABA receptors and transporters.
- TOLs colocalize with their cargo in different endocytic compartments in the root epidermis and in guard cells of stomata, where they potentially function in ABA-controlled stomatal aperture.
- Although the *tol2/3/5/6* quadruple mutant plant line is significantly more drought-tolerant and has a higher ABA sensitivity than control plant lines, it has no obvious growth or development phenotype under standard conditions, making the *TOL* genes ideal candidates for engineering to improved plant performance.

Introduction

The phytohormone abscisic acid (ABA) is involved in a variety of abiotic and biotic stress responses, plus aspects of plant growth and development, like root growth, stomatal closure, seed germination and dormancy (Finkelstein, 2013; Nakashima & Yamaguchi-Shinozaki, 2013). ABA elicits plant responses through the PYRABACTIN RESISTANCE1 (PYR1)/PYR1-LIKE (PYL)/REGULATORY COMPONENTS OF ABA RECEPTORS (RCAR) family of ABA receptors, which were initially reported as soluble proteins in the cytosol and nucleus (Ma *et al.*, 2009; Park *et al.*, 2009), but can also be recruited to the plasma membrane (PM) via the C2-DOMAIN ABA-RELATED (CAR) protein family (Rodríguez *et al.*, 2014; Diaz *et al.*, 2016). ABA-binding to the receptor is followed by interaction with and inactivation of clade-A PROTEIN PHOSPHATASE TYPE2Cs (PP2Cs), key negative regulators of the ABA signaling pathway (Weiner *et al.*, 2010). The formation of this complex relieves their inhibition on SUCROSE NON-FERMENTING1 RELATED KINASE2 (SnRK2), which phosphorylates specific protein targets,

including membrane ion channel-like SLOW ANION CHANNEL-ASSOCIATED1 (SLAC1) and transcription factors of the ABA INSENSITIVE5/ABA RESPONSIVE ELEMENT BINDING FACTOR (ABI5/ABF) family (Cutler *et al.*, 2010).

Modulation of ABA signaling occurs at the transcriptional, translational and posttranslational level, where ubiquitination plays a fundamental role in controlling stability of ABA signaling components by influencing their degradation to adjust and eventually cease this pathway. Turnover was shown via the 26S proteasome and the vacuole (Yu *et al.*, 2016b; Yu & Xie, 2017; Ali *et al.*, 2020), where main actors are E3 ligases, which confer target specificity for ubiquitination and act in the nucleus, cytosol and at the PM (Chen & Hellmann, 2013; Shu & Yang, 2017). Different E3 ligases can target the same substrates, likewise the same E3 ligase can ubiquitinate different proteins. Members of the RING FINGER OF SEED LONGEVITY1 (RSL1)/RING FINGER ABA-RELATED (RFA) E3 ligases family show distinct functions. RFA1 and RFA4, which reside in the nucleus and cytosol, ubiquitinate and cause the degradation of PYL4 via 26S proteasome (Fernandez *et al.*, 2020), whereas RSL1 can

ubiquitinate both PYR1 and PYL4 at the PM (Bueso *et al.*, 2014; Belda-Palazon *et al.*, 2016). PYL4, can be both K48- and K63-poly-ubiquitinated (Yu *et al.*, 2016a), nevertheless, it has not been conclusively demonstrated, which E3 ligases causes the differing chain types.

Ubiquitination of membrane-associated cargoes is a key signal for endosomal sorting and further transport to the vacuole for degradation via the Endosomal Sorting Complex Required for Transport (ESCRT) machinery (Isono & Kalinowska, 2017). This machinery is a conserved, multi-subunit membrane remodeling complex, which acts in recognition, concentration and sequestering of cargo into multivesicular bodies (MVB) and the membrane deforming events (Isono & Kalinowska, 2017; Gonzalez Solis *et al.*, 2022). The ESCRT-0 complex is required for initial targeting and concentration of ubiquitinated cargo and in recruiting the ESCRT-I (Bilodeau *et al.*, 2003). It represents a more recent addition and is not present in plants, but substituted for by the conserved TOM1-LIKE (TOL) protein family (Isono, 2020; Schwihla & Korbei, 2020), which function as multivalent ubiquitin receptors ensuring cargo delivery to the vacuole (Korbei *et al.*, 2013; Moulinier-Anzola *et al.*, 2020).

In plant cell suspension cultures, several components of the ESCRT machinery, including *TOLs* (in particular *TOL2* and *TOL5*), are highly upregulated in early drought stress responses (Alqurashi *et al.*, 2018). Furthermore, involvement of the ESCRT machinery in ABA signal modulation is evidenced by physical interaction of PYR/PYL/RCAR receptors with the plant-unique ESCRT subunits FYVE1 (Fab1, YOTB, Vac1 and EEA1)/FREE1 (FYVE DOMAIN PROTEIN REQUIRED FOR ENDOSOMAL SORTING1), the ESCRT-I subunit VACUOLAR PROTEIN SORTING 23A (VPS23A) and the ESCRT-associated protein ALG-2 INTERACTING PROTEIN-X (ALIX). ABA receptors, in particular PYR1 and PYL4, follow the endosomal trafficking route and are sorted via the ESCRT machinery into to the vacuole for degradation. Furthermore, *vps23a*, *alix-1* and several different *fyve1* mutants displayed increased sensitivity to ABA (Belda-Palazon *et al.*, 2016; Yu *et al.*, 2016a; Garcia-Leon *et al.*, 2019).

Endosomal trafficking also regulates turnover of transporters, like the ABA exporter ATP BINDING CASSETTE G25 (ABCG25), which controls ABA homeostasis (Kuromori *et al.*, 2010). Inhibition of clathrin-mediated endocytosis strongly reduced endocytosis of ABCG25 and exogenously applied ABA blocks turnover of ABCG25, leading to its accumulation at the PM (Park *et al.*, 2016). In addition, the interplay between recycling and degradation of ABCG25 is tightly regulated (Nguyen *et al.*, 2018; Liang *et al.*, 2022).

In this study, we show that distinct *TOLs* proteins play a role in modulating the ABA signaling pathway by affecting endosomal trafficking of core components of the ABA signaling and transport machinery. The *tol2/3/5/6* quadruple mutant has no obvious phenotype under standard conditions but is more drought-tolerant and has a higher ABA sensitivity than control plant lines. While *TOLs* are not involved in the ABA biosynthesis pathway, they affect the ABA signaling pathway where they function epistatic to VPS23A by influencing the stability of integral membrane proteins like ABA exporters, but also of the mostly cytoplasmic/nuclear ABA

receptors. Strikingly, *TOLs* colocalize with their conditional cargo in different endocytic compartments not only in the root epidermis but also in the guard cells of stomata, where they act as regulators of ABA responses, such as stomatal aperture. Based on our observations, we propose that *TOL2,3,5* and *6* additively function in attenuating ABA signaling through degradation of ubiquitinated ABA receptors and transporters.

Materials and Methods

Accession numbers

Arabidopsis Information Resource (TAIR) databases: PYR1 (At4g17870), PYL4 (AT2g38310), ABCG25 (AT1g71960).

Cloning procedure

Gateway cloning (Invitrogen) was used. Clones were confirmed by sequencing. Primers: Supporting Information Table S1. For *35S::GFP:PYR1*, *35S::RFP:PYR1*, *35S::GFP:PYL4* and *35S::GFP:ABCG25* open reading frames (ORF) of *PYR1*, *PYL4* and *ABCG25* were amplified from Col-0 cDNA. For *PYR1p::PYR1:GFP* a 1255 bp region upstream of PYR1 ORF together with PYR1 ORF was amplified from Col-0 gDNA. Entry clones were generated by BP reactions with pDONR221 and recombined by LR reactions into pB7WGF2 or pB7FWG,0 (GFP tag) and pB7WGR2 (RFP tag).

Growth conditions

All plant lines were of Col-0 ecotype. Surface sterilized seeds were plated on ½ MS plates (Murashige & Skoog, 1962), stratified 48–72 h in dark at 4°C and grown under long-day conditions (16 h : 8 h, light : dark) at 22°C with 125 μmol m⁻² s⁻¹ PPFD (Plant Photon Flux Density) light intensity and 50% relative humidity. *TOL* reporters were previously described in (Korbei *et al.*, 2013; Moulinier-Anzola *et al.*, 2020). To confirm homozygous progeny from crosses, plants were screened by genotyping PCR, digestion or sequencing according to primer combinations listed in Table S1 or as described in (Korbei *et al.*, 2013). Transgenic plants were generated by transformation of Flowering Col-0 with *Agrobacterium tumefaciens* using the floral dip method (Clough & Bent, 1998). Resulting T2 lines were screened for single transgene insertion sites. At least three independent transformants with similar results were characterized for each line. Plant lines: Table S2.

Drought assay

Same amount of soil (100 g) and water (40 ml) were used to prepare each pot (7 × 7 × 8 cm; 10 g). 4 DAG seedlings (nine/pot) were transferred to soil. Plants were kept in a closed plastic tray for 2 d. Drought treatment started at the third day. Pots were randomized daily to ensure equal growth conditions. Control plants were watered every second day. Drought conditions ended after 3 wk when the pots reached a weight of c. 50 g. The

plants were rehydrated for 2 h with water to a final weight of 150 g. After 3 d, pictures were taken to determine survival rate.

Thermal infrared (IR) imaging

Surface temperatures of rosette leaves from each plant line were examined with an IR camera (Model FLIR T1020) and thermal images were analyzed with FLIR Analysis Tool (RESEARCHIR Software v.4.30.2).

Quantification of stomatal size and aperture

8 DAG seedlings were harvested directly into 95% ethanol, after 2–3 h light exposure, fixed for 3–4 h and incubated for 10 min successively 70%, 50% and 20% ethanol and cleared overnight in 1 : 3 : 8; glycerol : water : chloral hydrate. Cotyledons were placed abaxial face upward and imaged with 20× objective. Per experiment, one image (taken at the same position) per cotyledon from 10 individuals were imaged. IMAGEJ was used for quantification of stomatal parameters: aperture index (opening of the pore in μm) and size index (length \times width of both guard cells in μm^2).

Germination and cotyledon greening assay

100 seeds per plant line were plated on $\frac{1}{2}$ MS plates supplemented with 0, 0.3 and 0.5 μM ABA (or 0 and 1 μM paclobutrazol). Radicle emergence was scored after 48 h, cotyledon greening was scored after 72 h as percentage of seedlings that developed green expanded cotyledons.

Root length measurement

20–40 seedlings (4 DAG) were transferred to new plates supplemented with 5 μM ABA or with solvent only. The root tip was marked at the starting point. After 4 d, plates were scanned and additional root growth measured (IMAGEJ).

ABA quantification

100 mg fresh weight of 7 DAG seedlings was extracted with methanol, water, acetic acid (80 : 19 : 1, v/v/v) containing internal standards (deuterium-labelled ABA). After centrifugation, the supernatant was dried in a vacuum evaporator and dissolved in 1% acetic acid and further purified by reverse-phase chromatography. The dried eluate was dissolved in 5% acetonitrile-1% acetic acid and separated by reverse phase UHPLC chromatography. ABA was analyzed with a Q-Exactive mass spectrometer (Orbitrap detector; Thermo Fisher Scientific, Waltham, MA, USA) by targeted Selected Ion Monitoring (SIM).

Confocal laser scanning microscopy (CLSM)

Images were generated from 6 DAG seedlings using a Leica SP5 or Zeiss LSM980. The following conditions were used: 488 nm (GFP, BCECF-AM (2',7'-bis-(2-carboxyethyl)-5-(and-6)-carboxyfluorescein-acetoxymethyl ester), 514 nm (Venus) and

561 nm (RFP and FM4-64)). Settings were kept constant to allow for comparison of specific reporter proteins. Images were taken in the same region from at least seven individuals and equally processed for brightness and contrast using Affinity Designer. 3D reconstruction and surface rendering of the BCECF-AM-stained vacuoles, from 16 z-Stack Images (0.5 μm step size). The data were processed with IMAGEJ, using the Surface rendering option in the 3D viewer plugin. Drugs and stains: Table S3.

Global Ubiquitination assay and total Protein Extraction of seedlings or roots was performed as described in (Moulinier-Anzola *et al.*, 2020). Antibodies used in this study: Table S4.

Immunoprecipitation (GFP-Trap)

7 DAG seedlings were sprayed with solvent or 100 μM ABA, harvested after 4 h (500 mg), shock frozen and pulverized with a Retsch mill. 2 $\mu\text{l mg}^{-1}$ of cold extraction buffer (10% glycerol, 25 mM Tris-HCl pH 7.4, 1 mM EDTA, 150 mM NaCl, 2% polyvinylpyrrolidone, 1 mM DTE, 0.1% Nonidet P-40 [NP-40], cOmplete™, Mini, EDTA-free Protease-Inhibitor-Cocktail (Roche) and 20 mM N-ethylmaleimide) was added, incubated end-over-end (0.0193 g) for 30 min at 4°C, centrifuged for 15 min at 21 130 $\text{g}/4^\circ\text{C}$ and the supernatant transferred to a new tube containing 25 μl slurry of equilibrated GFP-TRAP® Agarose beads (Chromo Tek, Munich, Germany), incubated at 4°C end-over-end (0.0193 g) for 90 min, centrifuged at 587 g at 4°C. Beads were washed 2× with 1 ml cold IP buffer (10% glycerol, 25 mM Tris-HCl pH 7.4, 1 mM EDTA, 150 mM NaCl and 0.1% NP-40) and 1× with 1 ml cold wash buffer (50 mM NaCl and 20 mM Tris-HCl pH 7.4), proteins were eluted by adding 100 μl 1× Laemmli buffer and boiling at 95°C for 10 min.

Quantitative real-time polymerase chain reaction analysis

7 DAG seedlings were sprayed with 10 μM ABA or solvent, harvested after 1 h and total RNA was extracted using SV Total RNA extraction Kit (Promega). cDNA was generated with iScript reverse transcriptase kit (Bio-Rad). Primers: Table S1.

Results

A distinct *tol* quadruple mutant tolerates drought conditions, has a higher foliar temperature and reduced stomatal aperture

Deficiencies in sorting and vacuolar degradation of ubiquitinated PM proteins were previously observed in *tolQ*, a mutant lacking five different *TOLs* (*TOL2,3,5,6* and *9*), with severe pleiotropic phenotypes (Korbei *et al.*, 2013; Moulinier-Anzola *et al.*, 2020), which hampers clear-cut characterization of *TOL* function. Thus, we aimed at assessing involvement of *TOLs* in additional signaling pathways in less detrimental genetic backgrounds. Since the endocytic trafficking pathway, especially the ESCRT machinery, modulates turnover of ABA receptors and plays a role in ABA

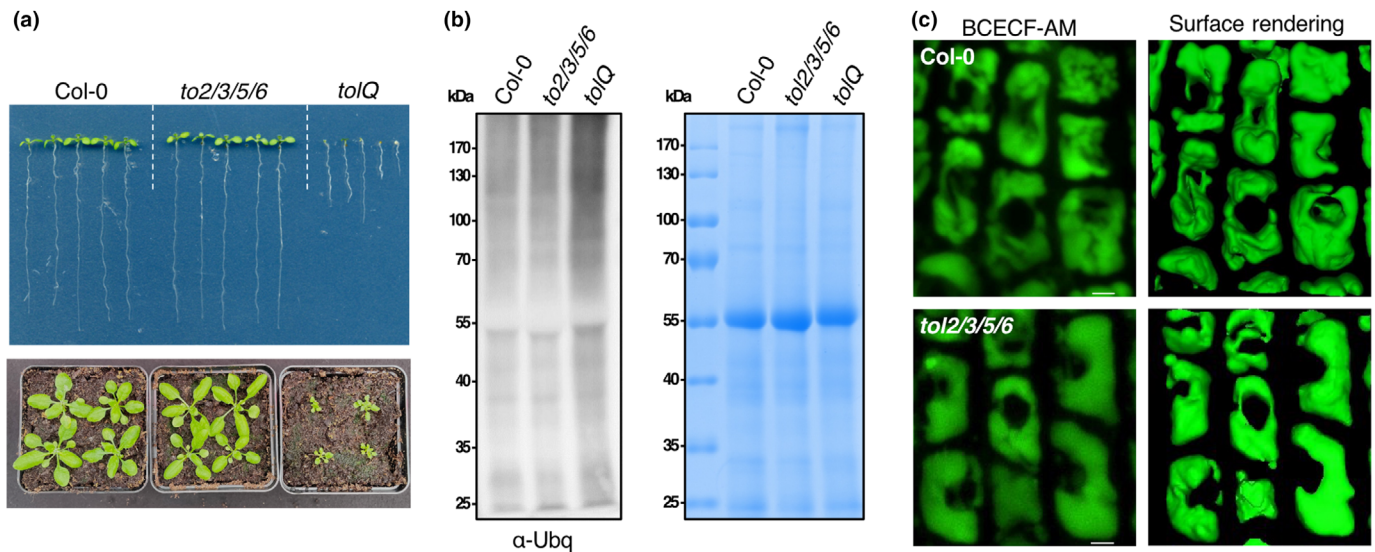


Fig. 1 Loss of *TOL* 2,3,5 and 6 genes results in no general phenotypical alterations. (a) Phenotypic comparison of wild-type (Col-0), *tol2/3/5/6* and *tolQ* plant lines at 7 d after germination (DAG) (upper panel) and 20 DAG (lower panel). (b) Accumulation of ubiquitin conjugates in Col-0, *tol2/3/5/6* and *tolQ* plant lines. Total protein extracts of adult leaves of 35 DAG plants were subjected to SDS-PAGE and immunoblotting using an anti-ubiquitin antibody (α -ubq, left panel) or Coomassie staining (right panel) as loading control. (c) Root epidermis cells of 6 DAG seedlings were stained with BCECF-AM for 1 h and analyzed using CLSM (left panels). 3D reconstruction analysis by surface rendering on z-stack images (right panels) show no significant morphological differences between Col-0 and *tol2/3/5/6* vacuoles. Bar, 5 μ m.

signaling (Belda-Palazon *et al.*, 2016; Yu *et al.*, 2016a; Garcia-Leon *et al.*, 2019), we investigated the contribution of the *TOLs* to ABA responses. We examined different single and higher-order *tol* mutant combinations for their sensitivity to ABA and tolerance to drought.

As no obvious, strong ABA-related phenotypes were found in single and double mutants, we tested a higher order quadruple *tol* mutant plant line, *tol2-1/tol2-1 tol3-1/tol3-1 tol5-1/tol5-1 tol6-1/tol6-1 (tol2/3/5/6)*. When grown under standard conditions it lacked any apparent vegetative or reproductive phenotypes in the seedling and adult stage, which is in stark contrast to *tolQ* additionally deficient in *TOL9* (Fig. 1a). Moreover, at a protein level *tol2/3/5/6* failed to show the same ectopic accumulation of ubiquitinated cargoes as described for *tolQ* (Moulinier-Anzola *et al.*, 2020), indicative of comparably weak, perhaps more specific defects in *tol2/3/5/6* (Fig. 1b). Furthermore, we assessed the vacuolar morphology of Col-0 and *tol2/3/5/6* seedlings using BCECF-AM, a dye that labels acidic compartments, such as vacuoles and detected no difference (Fig. 1c).

Remarkably though, the *tol2/3/5/6* plant line exhibited an increased tolerance towards drought conditions, similar to phenotypes described for the drought-tolerant *hab1-1abi1-2* double mutant, deficient in two PP2Cs: ABA-INSENSITIVE1 (ABI1) and HYPERSENSITIVE TO ABA1 (HAB1) (Saez *et al.*, 2006) as well as a substantially increased drought stress recovery rate, when compared either to wild-type (WT) or the highly drought susceptible *open stomata2-2 (ost2-2)* (Merlot *et al.*, 2007) (Fig. 2a). Furthermore, drought-induced wilting phenotypes became apparent very delayed in flowering *tol2/3/5/6* plants, compared to WT (Fig. S1a).

Altered leaf temperature, analyzed by thermal infrared imaging, is an established readout for analysis of mutants with stomata opening deficiencies, causing alterations in leaf surface temperature through alterations in transpiration (Merlot *et al.*, 2002). In adult *tol2/3/5/6* plants we observed a significantly higher foliar temperature than in WT controls, which was even more pronounced in *hab1-1abi1-2*. Conversely *ost2-2* displayed a lower foliar temperature, reflecting increased stomatal transpiration of this mutant (Merlot *et al.*, 2007) (Fig. 2b). Furthermore, stomatal aperture and size of guard cells in stomata of *tol2/3/5/6* cotyledons of seedlings were significantly smaller than WT counterparts (Figs 2c, S1c), consistent with our observations revealing differing foliar temperatures in the adult plants.

Collectively, our observations suggest a role for *TOL2,3,5* and *6* in drought stress-induced adaptive responses.

tol2/3/5/6 is hypersensitive to ABA

Drought responses in general, as well as variations in stomatal aperture in particular, are decisively influenced by ABA signaling, which led us to test the responsiveness of *tol2/3/5/6* to ABA treatment (Munemasa *et al.*, 2015). After 1 h of ABA or mock treatment of *tol2/3/5/6* and WT seedlings, we assessed transcript levels of ABA-responsive genes by quantitative real-time polymerase chain reaction using the stress-responsive gene *RESPONSIVE TO DESICCATION 29A (RD29A)* as well as transcription factor *ABA INSENSITIVE 5 (ABI5)* (Nakashima *et al.*, 2006; Zhao *et al.*, 2020). While no difference can be seen without treatment, ABA-induced upregulation of these genes was more pronounced in *tol2/3/5/6* compared to the WT, (Fig. 2d), indicating increased

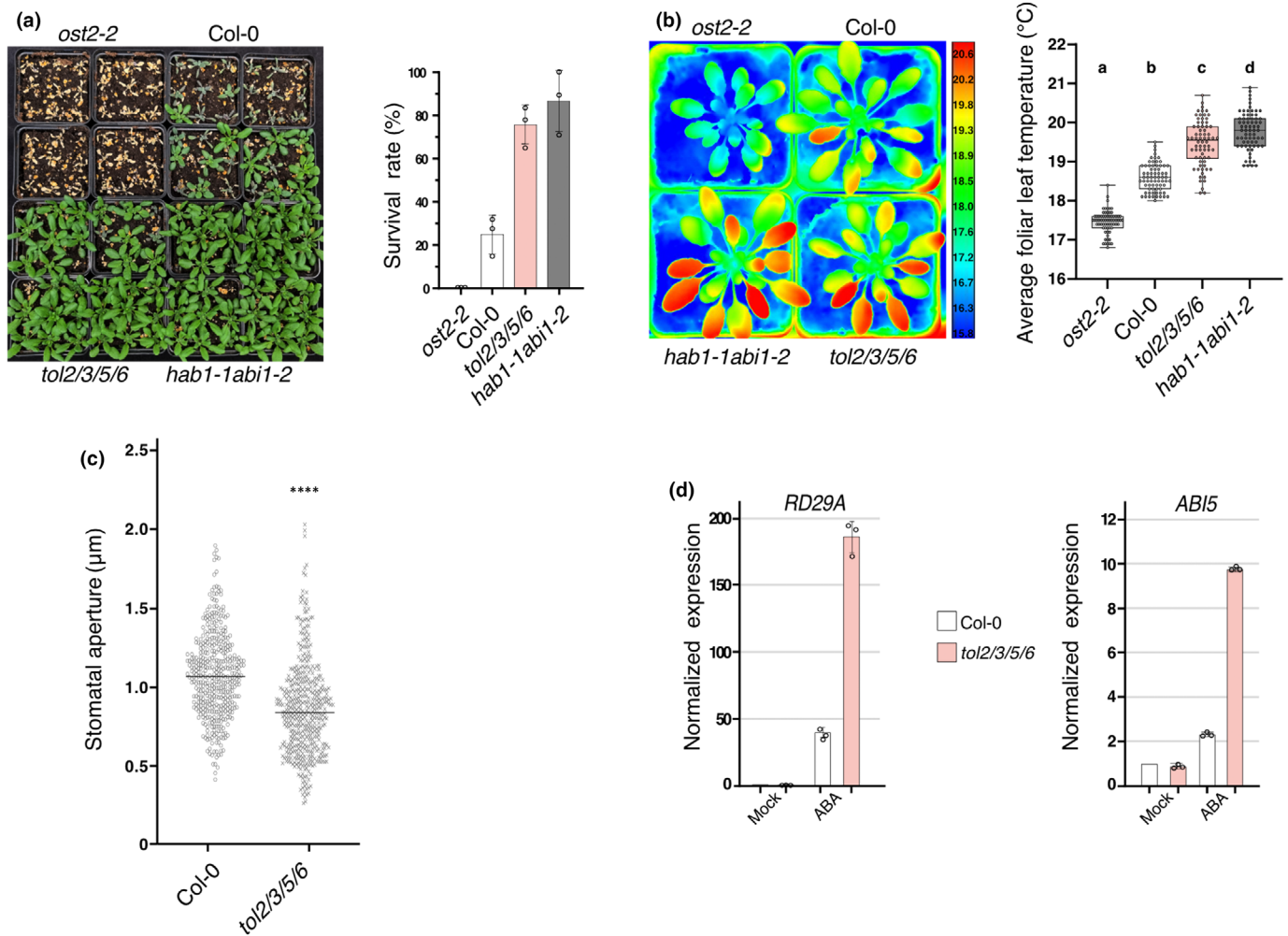


Fig. 2 The *tol2/3/5/6* plant line shows higher drought tolerance and ABA-related defects. (a) Assessment of the survival rate of adult plants of *Col-0*, *tol2/3/5/6*, *hab1-1abi1-2* and *ost2-2* genotype after 3 wk of drought stress. A representative picture was taken directly before (see Supporting Information Fig. S1b) and 3 d after rewatering and the survival rate was determined. Data shown in the diagram on the right side represents the mean values \pm SD of independent experiments ($n = 3$ with 36 plants per genotype). (b) Monitoring the foliar leaf temperature by thermal IR imaging of 26 DAG *Col-0*, *tol2/3/5/6*, *hab1-1abi1-2* and *ost2-2* plant lines. To assess the leaf surface temperature individual rosette leaves for each plant line were measured. Correspondence between false colors and temperature is shown to the right. Values of foliar leaf temperature measurements ($n = 70$ for each plant line) are represented as boxplots with median. The shown data was analyzed by one-way ANOVA with *post hoc* Tukey HSD test. Different letters above each bar indicate statistically significant differences. The experiments were repeated three times with similar results. (c) Stomatal aperture (width of the pore) measurements of wild-type (WT) and *tol2/3/5/6* cotyledon leaves. Individual values are shown with median ($n > 450$). The experiments were repeated three times with similar results. ****, $P < 0.0001$ (student's *t*-test) with respect to WT in same experimental conditions. (d) Relative expression level analyses of *RD29A* and *ABI5* induced by ABA. Total RNA was extracted from seedlings of 7 DAG seedlings of *Col-0* and *tol2/3/5/6* treated with 10 μ M ABA or mock for 1 h and cDNA was analyzed by quantitative real-time polymerase chain reaction using gene-specific primers. The expression was normalized against the Alpha subunit of ELONGATION FACTOR 1 ALPHA (EF1 Alpha) gene and the expression level of the WT in mock treatment was arbitrarily set to 1. Error bars represent \pm SD from three technical replicates from one experiment, and the experiments were performed three times with similar results.

sensitivity to ABA. We furthermore tested the *tolQ* plant line and found although this also showed increased sensitivity to ABA, it also exhibits strongly increased basal expression levels (Fig. S2a), underlining the severe defects associated with this mutant. We also tested all triple *tol* mutant combinations contained in *tol2/3/5/6*, for enhanced response to ABA to assess if all four *TOL* genes are essential for the response. A similar hypersensitive effect can be seen using *tol2/3/5*, *tol2/3/6*, *tol2/5/6* and *tol3/5/6*, but none to the same extent as *tol2/3/5/6* (Fig. S2b). Thus, our findings indicate that

these four *TOL* genes act redundantly in transcriptional ABA response, though potentially to different degrees.

Given their apparent function in the control of ABA responses and previous expression analysis that points toward overlapping but also distinct functions of the *TOLs* (Moulinier-Anzola *et al.*, 2014), we tested if transcription of individual *TOL* genes is responsive to ABA treatment. We found that *TOL 2,3,5* and *6* are all transcriptionally induced by ABA, with the strongest up-regulation for *TOL5* (Fig. S2c), while *TOL9* was not upregulated

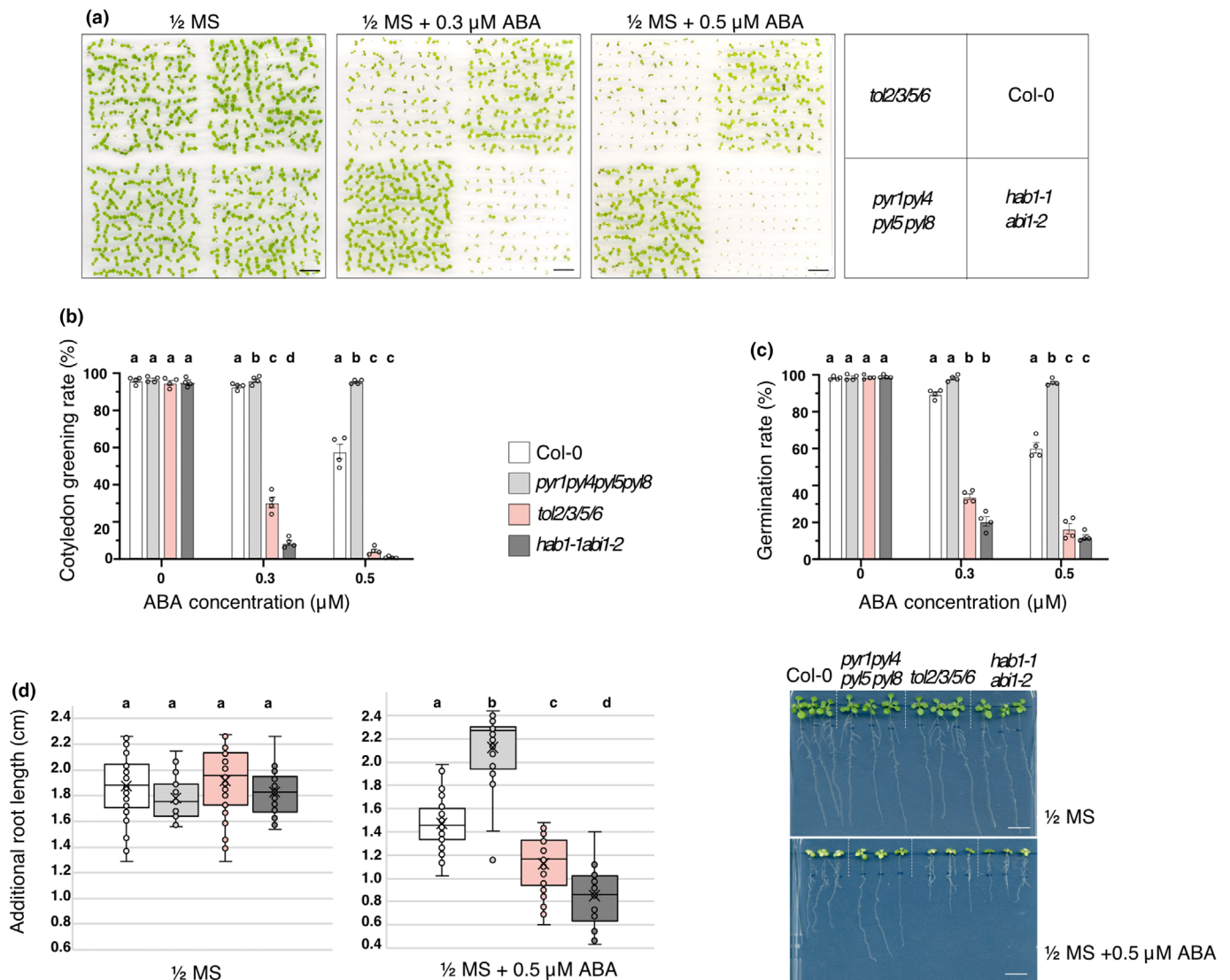


Fig. 3 *tol2/3/5/6* is hypersensitive to ABA. (a) Seeds of each plant line Col-0, *tol2/3/5/6*, *hab1-1abi1-2* and *pyr1py4py5py8* were germinated on media supplemented with 0.3 or 0.5 μM ABA or just solvent as control. After 4 d a representative picture of each plate was taken. A pictogram of the plating scheme is depicted on the right side. Bars: 1 cm. (b) Cotyledon greening rates were scored after 72 h. Data shown represent the mean values ± SD of independent experiments ($n = 4$ with 100 seeds plated and scored per genotype, condition and replicate). (c) Germination rate was scored after 48 h, data represents mean values ± SD of independent experiments ($n = 4$ with 100 seeds plated and scored per genotype, condition and replicate). (d) Col-0, *tol2/3/5/6*, *hab1-1abi1-2* and *pyr1py4py5py8* seedlings (4 DAG) were transferred from control plates to plates supplemented with 5 μM ABA- or mock-treated. After 4 d, the additional grown root was measured. Boxplots of additional root length ($n = 9-14$ seedlings). Center line, median. The experiment was conducted three times with similar results. Photograph of representative plants analyzed are shown in the right panel. Bars: 1 cm. Data shown in b, c and d was analyzed by one-way ANOVA with *post hoc* Tukey HSD test. The different letters indicate statistically significant differences.

after 1 h and only slightly after 4 h. This underlines potential mechanistic links between these four specific TOLs and ABA-dependent stress responses.

ABA hypersensitivity of *tol2/3/5/6* is similar to a PP2C double mutant

To examine roles for TOLs in ABA responses, we investigated selected ABA-regulated growth responses like ABA-mediated inhibition of seed germination, cotyledon greening rate and root

growth. We compared *tol2/3/5/6* to WT (Col-0), the quadruple *pyr1py4py5py8* ABA receptor mutant plant line (Park *et al.*, 2009; Gonzalez-Guzman *et al.*, 2012) as ABA-insensitive control and the *hab1-1abi1-2* double mutant as a reference for the ABA-hypersensitive phenotype (Saez *et al.*, 2006). For the cotyledon greening assays, we scored the percentage of seedlings with emerged green cotyledons after 3 d on plates with increasing ABA concentration (Fig. 3a,b). In THE absence of exogenous ABA, no significant differences can be seen in the different plant lines. By contrast, *hab1-1abi1-2* seedlings displayed dosage-

dependent reduced cotyledon greening on ABA plates, indicating enhanced sensitivity to ABA. The same was discernible for *tol2/3/5/6*, albeit to a slightly lower degree, which can be seen particularly well when assessing the effects of lower ABA concentrations. Contrarily and as expected, the *pyr1pyl4pyl5pyl8* ABA receptor mutant was markedly less affected by ABA than WT (Fig. 3a,b).

Comparable responses were observed when scoring the germination rate, where we assessed radicle emergence after 2 d (Fig. 3c). During seed germination, ABA signaling is desensitized (Shu *et al.*, 2016), thus germination on plates supplemented with the growth regulator is inferior in hypersensitive ABA signaling mutants such as *hab1-1abi1-2* and is less severely affected in *pyr1pyl4pyl5pyl8*. While a large portion of the WT seeds still germinated on medium supplemented with increasing concentrations of ABA, a substantially smaller fraction of the *tol2/3/5/6* seeds did so (Fig. 3c). Enhanced sensitivity to ABA during germination indicates that loss of *TOLs* leads to enhanced ABA responses. Corresponding germination assays were performed with all triple *tol* mutant combinations, to once again assess the contribution of the individual *TOL* genes to the overall enhanced ABA sensitivity of *tol2/3/5/6*. We could confirm the additivity *TOL* functions as all triple mutants react more sensitively to ABA than WT, nevertheless not as strongly as *tol2/3/5/6* (Fig. S2d). The *tol2/3/6* plant line responded most similarly to the control, indicating that strongest effects are caused by a loss of *TOL5*, nevertheless only in combination with additional mutant *TOL* loci.

In these two assays, loss of *TOL* function exerts effects similar to a loss of PP2Cs and related findings were made when assessing the effect of ABA on root growth. For this, seedlings were grown on regular medium then transferred to medium with or without ABA. When comparing the additional root growth after 4 d on ABA-supplemented plates with controls, *tol2/3/5/6* shows increased ABA sensitivity similar to *hab1-1abi1-2*, albeit not as pronounced, while *pyr1pyl4pyl5pyl8* was even less sensitive than Col-0 (Fig. 3d).

In summary, these results demonstrate that *tol2/3/5/6* is ABA-hypersensitive, overall consistent with a function of selected *TOLs* as negative regulators of ABA signaling. Furthermore, *TOL2,3,5* and *6* are induced by ABA and exhibit redundant, but additive roles, where *TOL5* seems to play the most prominent role for ABA responses.

TOLs do not play a significant role in ABA biosynthesis

The abovementioned observations link *TOL* genes to the regulation of ABA responses in *Arabidopsis thaliana* L. Heynh. To investigate potential functions of *TOL* proteins in ABA metabolism, we assessed total ABA content in Col-0 and *tol2/3/5/6* seedlings, which showed no significant deviation, demonstrating that ABA homeostasis is not notably affected in *tol2/3/5/6* (Fig. 4a). This is supported by quantitative real-time polymerase chain reaction results (Fig. 2d), where *RD29A* and *ABI5* levels are not significantly altered in *tol2/3/5/6* compared to Col-0 without treatment, implying that there is no constitutive increase in the ABA response.

Next, we crossed *tol2/3/5/6* into the moderately strong *aba1-6* ABA biosynthesis mutant affected in *ABA DEFICIENT1 (ABA1)* (Barrero *et al.*, 2005), which is in the same genetic background as the mutant *tol* lines, followed by phenotypic analysis of the resulting mutant combination. ABA biosynthesis mutants show a higher germination rate on plates supplemented with the gibberellin (GA) biosynthesis inhibitor paclobutrazol (PAC), since they require lower amounts of GA to germinate (Leon-Kloosterziel *et al.*, 1996). We confirmed the PAC-resistant germination phenotype of *aba1-6* (Barrero *et al.*, 2005) and furthermore observed comparable PAC-induced responses of the *aba1-6 tol2/3/5/6* quintuple mutant (Fig. 4b). WT showed the expected reduced germination rate on PAC-supplemented plates, which was even more pronounced for *tol2/3/5/6* (Fig. 4b). This indicates that a loss of four *TOL* genes does not affect ABA biosynthesis, as GA deprivation through PAC treatment still inhibits germination. Furthermore, the enhanced PAC-mediated inhibition of *tol2/3/5/6* seed germination compared to Col-0 is in agreement with the ABA-hypersensitive response.

In the germination assay on plates with increasing ABA concentration, *aba1-6* showed no alterations when compared to WT, while only a smaller fraction of *tol2/3/5/6* seeds germinated on ABA-supplemented growth medium, and *aba1-6 tol2/3/5/6* seeds behaved just like the *tol2/3/5/6* parental line (Fig. 4c). This indicates that the pathway affected by the *TOLs* is not significantly influenced by ABA biosynthesis. Additionally, no additive phenotype neither at vegetative (Fig. 4d) nor at the reproductive stage (Fig. S3a) were observed in the development of *aba1 tol2/3/5/6* individuals, when compared to the parental lines.

TOLs play a role in ABA signaling by influencing ESCRT-mediated trafficking decisions

To study genetic relationships between loss of *TOL* function and negative regulators of ABA signaling, we combined informative mutants by crossing. In the *hab1-1abi1-2 tol2/3/5/6* hextuple mutant, a developmental delay can be observed during vegetative (Fig. 4d) and reproductive stages (Fig. S3a), when compared to the parental lines. In the cotyledon greening assay, in the absence of exogenous ABA, *hab1-1abi1-2, tol2/3/5/6* and *hab1-1abi1-2 tol2/3/5/6* showed a cotyledon greening rate similar to WT. However, in the presence of exogenous ABA, the tested mutant combinations were more sensitive to ABA than Col-0, with *tol2/3/5/6* showing a weaker effect than *hab1-1abi1-2*. For the *hab1-1abi1-2 tol2/3/5/6* hextuple mutant, we observed the strongest ABA responsiveness among the mutant lines tested (Fig. 4e), indicating that *TOLs* and PP2Cs both contribute to ABA responsiveness, nevertheless not with completely overlapping functions.

As components of the ESCRT machinery have already been linked to ABA responses (Belda-Palazon *et al.*, 2016; Yu *et al.*, 2016a; Garcia-Leon *et al.*, 2019), we assessed if *TOLs* could impact on ABA responses via their demonstrated function in endocytic sorting to the vacuole. To test genetic interaction of the relevant *TOL* genes with the ESCRT-I subunit VPS23A, which directly interacts with both *TOL2* and *TOL6* (Moulinier-Anzola *et al.*, 2020), we crossed *tol2/3/5/6* with a null mutant of

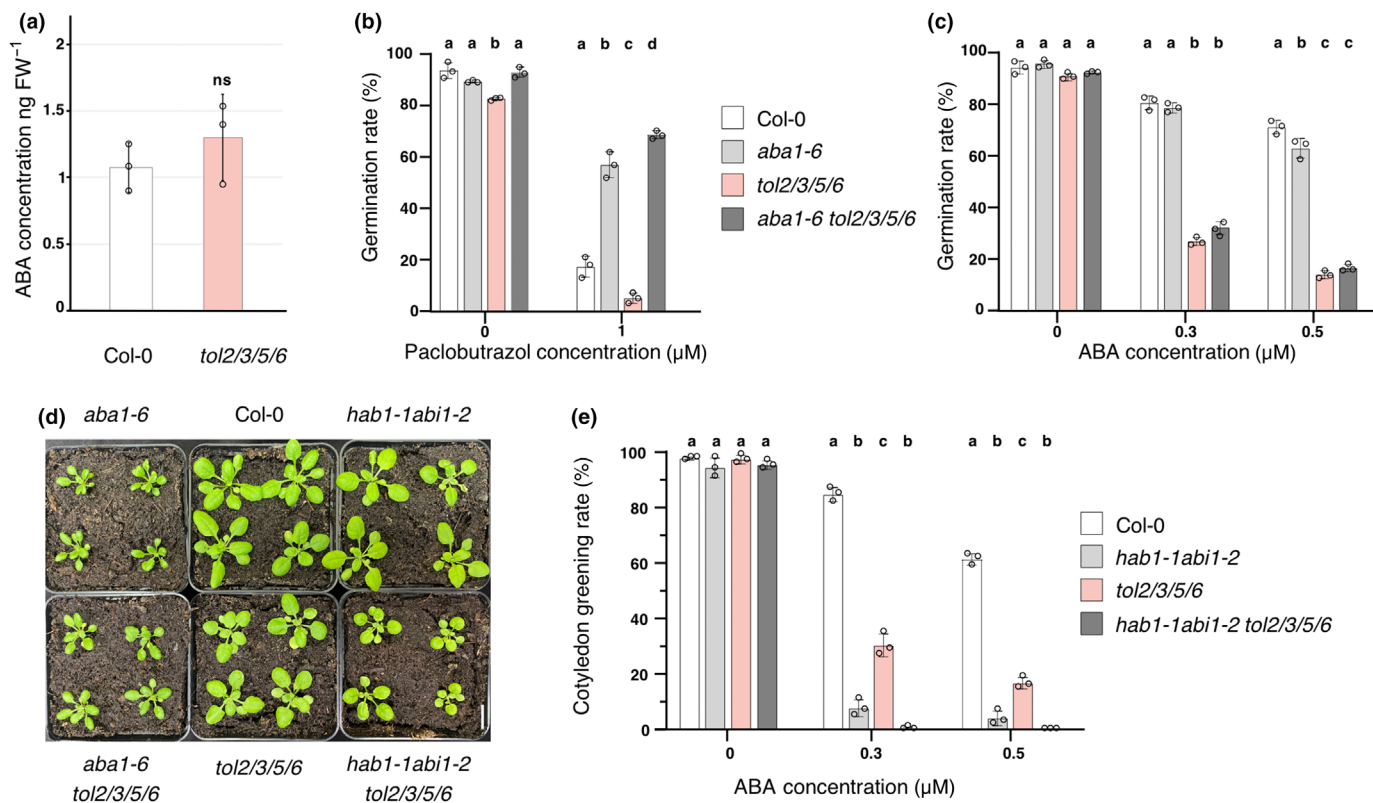


Fig. 4 TOLs do not play a significant role in ABA biosynthesis but a potential role in ABA signaling. (a) Col-0 and *tol2/3/5/6* seedlings grown on $\frac{1}{2}$ MS media were collected to measure ABA ($n = 3$). Data represents mean \pm SD of three independent experiments ABA concentration measurements ns indicates no significant difference by *t*-test. (b) Seeds of Col-0, *tol2/3/5/6*, *aba1-6* and *aba1-6 tol2/3/5/6* were plated on $\frac{1}{2}$ MS media supplemented with or without 1 μ M paclobutrazol. The germination rate was scored after 48 h. Data represents mean values \pm SD of independent experiments ($n = 3$; with 100 seeds plated and scored per genotype, condition and replicate). (c) Seeds of the abovementioned plant lines were germinated on $\frac{1}{2}$ MS media supplemented with 0.3 or 0.5 μ M ABA or just solvent as control. The germination rate of the seeds was scored after 48 h. Data represents mean values \pm SD of independent experiments ($n = 3$; with 100 seeds plated and scored per genotype, condition and replicate). (d) Phenotypes of plants lines Col-0, *tol2/3/5/6*, *aba1-6*, *aba1-6 tol2/3/5/6*, *hab1-1abi1-2* and *hab1-1abi1-2 tol2/3/5/6* at 21 DAG. Bar, 1 cm (e) Seeds of Col-0, *tol2/3/5/6*, *hab1-1abi1-2* and *hab1-1abi1-2 tol2/3/5/6* plant lines were germinated on $\frac{1}{2}$ MS media supplemented with 0.3 or 0.5 μ M ABA or just solvent as control. Cotyledon greening rates were scored after 72 h. Data shown represent the mean values \pm SD ($n = 3$; with 100 seeds plated and scored per genotype, condition and replicate). Data shown in b, c and e were analyzed by one-way ANOVA with *post hoc* Tukey HSD test. The different letters above each bar indicate statistically significant differences.

VPS23A termed *vps23.1-3* (Nagel *et al.*, 2017). While both parental lines resembled the WT, the *vps23.1-3 tol2/3/5/6* pentuple mutant showed a mild developmental defect during the vegetative and reproductive stages (Figs 5e, S3b).

We observed hypersensitivity to ABA of *vps23.1-3* in the cotyledon greening assay (Fig. 5a,b), the seed germination assay (Fig. 5c) as well as in ABA-responsive root growth (Fig. 5d). Remarkably though, *tol2/3/5/6* was significantly more sensitive to ABA in all the assays. The *vps23.1-3 tol2/3/5/6* pentuple mutant showed ABA sensitivity similar to *tol2/3/5/6* (Fig. 5), indicating that loss of these four *TOL* genes is epistatic over loss of *VPS23A* in ABA signaling. For that reason, TOLs function in mediating ABA responses could be upstream of *VPS23A*, jointly guiding cargo transport to the vacuole for degradation upon ABA treatment, as has been shown for *VPS23A* modulating steady-state levels of ABA receptors *PYL4* and *PYR1* (Yu *et al.*, 2016a).

To summarize, selected TOLs do not impact on overall ABA homeostasis but rather on ABA signaling, indicated by their

genetic interaction with essential effectors. Such TOL-mediated signaling likely involves trafficking decisions impacting on steady-state levels of ABA signaling components via the ESCRT machinery, with TOLs acting upstream of the ESCRT-I subunit *VPS23A*.

ABA receptors and transporters localize to endosomal compartments

To address participation of TOL proteins in trafficking of elements of the ABA signaling machinery, we constructed FP-tagged ABA receptors of the monomeric *PYL4* and the dimeric *PYR1* receptors, previously shown to be sorted via the ESCRT machinery for degradation (Belda-Palazon *et al.*, 2016; Yu *et al.*, 2016a; Garcia-Leon *et al.*, 2019). Furthermore, we generated a reporter for the ABA exporter *ABCG25*, which regulates cellular ABA homeostasis (Kuromori *et al.*, 2010) and is also subjected to endocytosis and vacuolar degradation (Park *et al.*, 2016; Nguyen

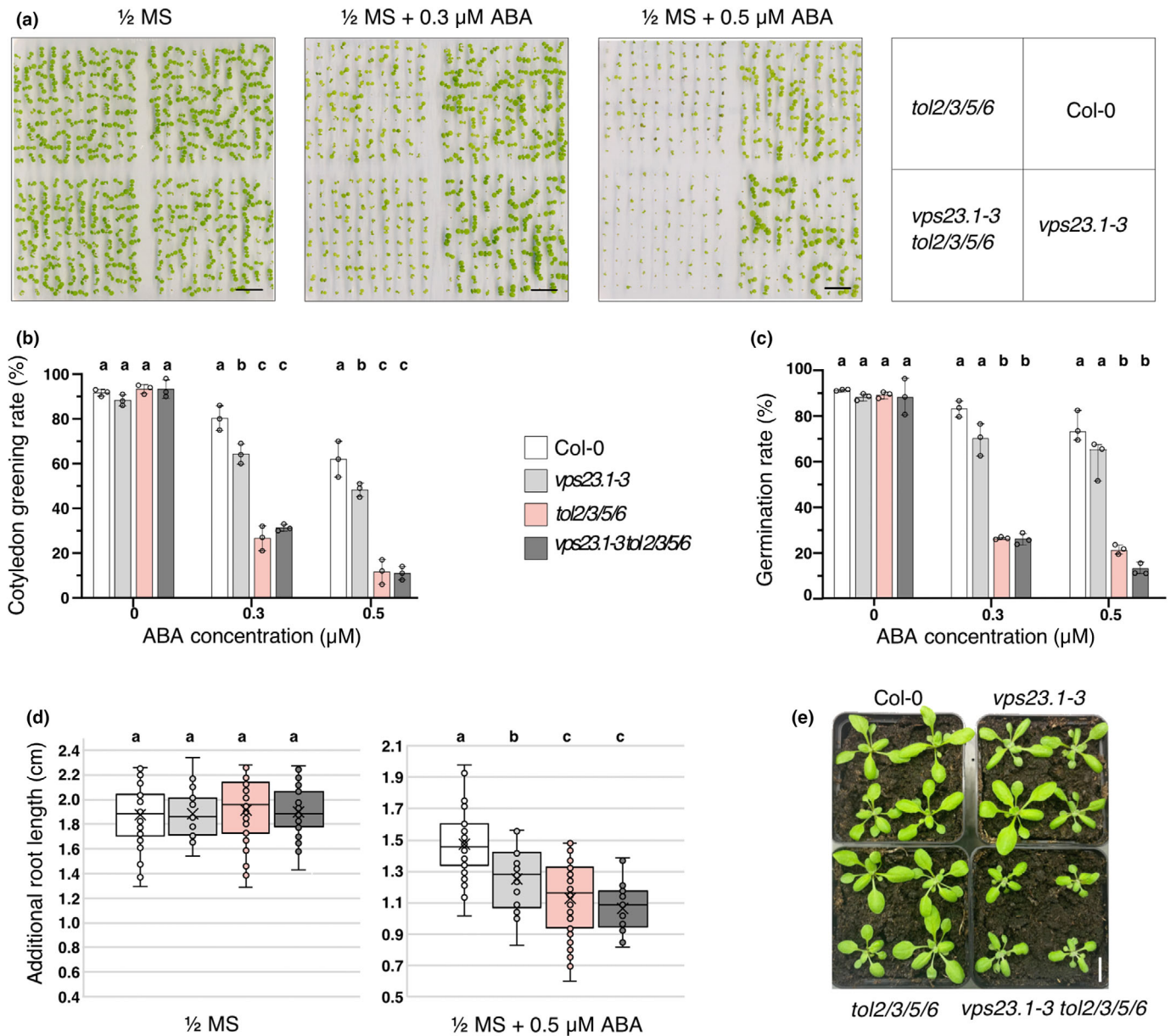


Fig. 5 Epistatic relationship between *TOL2,3,5,6* and *VPS23A* in ABA signaling. (a) Seeds of each plant line Col-0, *tol2/3/5/6*, *vps23.1-3* and *vps23.1-3 tol2/3/5/6* were germinated on media supplemented with 0.3 or 0.5 μM ABA or just solvent as control. After 4 d a representative picture of each plate was taken. A pictogram of the plating scheme is depicted on the right side. Bars: 1 cm. (b) Cotyledon greening rates were scored after 72 h. Data shown represent mean values ± SD of independent experiments ($n = 3$; with 100 seeds plated and scored per genotype, condition and replicate). (c) Germination rate was scored after 48 h. Data represents mean values ± SD of independent experiments ($n = 3$; with 100 seeds plated and scored per genotype, condition and replicate). (d) Col-0, *tol2/3/5/6*, *vps23.1-3* and *vps23.1-3 tol2/3/5/6* seedlings (4 DAG) were transferred from control plates to plates supplemented with 5 μM ABA- or mock-treated. After 4 d, the additional grown root was measured. Boxplots of additional root length ($n = 9-14$ seedlings). Center line, median. The experiment was conducted three times with similar results. Data shown in b, c and d was analyzed by one-way ANOVA with *post hoc* Tukey HSD test. The different letters indicate statistically significant differences. (e) Phenotypes of abovementioned plants lines at 21 DAG. Bar, 1 cm.

et al., 2018). In addition to stable *Arabidopsis* lines expressing RFP:PYR1, GFP:PYR1, GFP:PYL4 and GFP:ABCG25 under control of the 35S promoter we constructed a plant line expressing PYR1:GFP under its endogenous promoter. Confocal laser scanning microscopy (CLSM) was used to visualize subcellular localization of reporter signals in root meristem cells co-stained

with the lipophilic membrane dye FM4-64, a tracer of endomembrane compartments. This revealed that GFP-tagged PYR1 and PYL4 localized mostly in the cytoplasm and nucleus (Fig. S4a-c, left panels) while GFP:ABCG25 localized to the PM and showed additional punctate intracellular signals overlapping with FM4-64 signals, demarcating early endosomal structures

(Fig. S4d, left panels, white arrows) (Liang *et al.*, 2022). Furthermore, localization of PYR1:GFP expressed under its endogenous promoter showed the same localization in meristematic root cells, as when expressed under the strong 35S-promoter with an N-terminal GFP tag (Fig. S4a,b). To further ascertain the functionality of the reporters, we introduced a 35S::GFP:PYR1 plant line into *pyr1pyl4pyl5pyl8*, which caused rescue of the hyposensitive germination phenotype of this ABA receptor quadruple mutant (Fig. S5).

Next, we perturbed trafficking to the vacuole with the drug wortmannin (Wm), which inhibits phosphatidylinositol kinases acting in MVB formation (Robinson *et al.*, 2008), resulting in enlarged MVBs termed Wm bodies. Endosomal origin of the observed Wm bodies was confirmed by their staining with the endocytic tracer FM4-64. When testing overexpression lines as well as *PYR1p::PYR1:GFP* lines, we observed an accumulation of GFP:PYL4, GFP:PYR1, PYR1:GFP and GFP:ABCG25 signals in FM4-64-stained Wm bodies (Fig. S4 right panels), as described previously for *PYL4* and *ABCG25* (Belda-Palazon *et al.*, 2016; Yu *et al.*, 2016a; Nguyen *et al.*, 2018). This indicates, that a fraction of these proteins is constitutively targeted to the vacuole for degradation. Once again, neither the positioning of the GFP tag nor the reporter gene overexpression altered this localization, supporting the notion that ABA receptor proteins are indeed subject to continuous vacuolar turnover.

In planta colocalization studies of TOLs with ABA receptors and transporters in endosomal structures

To show that TOLs play a role in the initial steps of the downregulation of ABA transporters and receptors, we generated crosses of plant lines overexpressing FP-tagged PYR1 with lines expressing VENUS- or mcherry-tagged TOL2,3,5 and 6 under their endogenous promoter as well as plant lines overexpressing RFP-tagged PYL4 or ABCG25 with TOL5:VENUS-expressing lines. Subsequently, we assessed colocalization in root epidermal cells using CLSM. We mainly focused on *TOL5*, as this locus showed the most pronounced single-gene effect in mediating ABA responses (Fig. S2c). Furthermore, we assessed the functionality of the *TOL5* reporter gene in the *tol2/3/5/6* and *tol5-1* background in the germination assay. *Tol5-1 TOL5p::TOL5:VENUS* shows a germination rate similar to the WT, when germinated on increasing ABA concentrations, while *TOL5p::TOL5:VENUS* expressed in *tol2/3/5/6* results in better germination, when compared to *tol2/3/5/6* controls (Fig. S6).

In mock-treated root meristem cells TOL5:mcherry as well as TOL2, TOL3, TOL5 and TOL6 tagged with VENUS localized as reported previously (Korbei *et al.*, 2013; Moulinier-Anzola *et al.*, 2020), overlapping with PYR1 and PYL4 in the cytoplasm (Figs 6a, S7).

To learn about crosstalk between TOLs and ABA transporters and receptors in intracellular sorting, we pharmacologically interfered with endosomal trafficking to induce mislocalization of reporter proteins in endosomal sorting structures. The fungal toxin Brefeldin A (BFA) targets GTP-exchange factors of ARF GTPases (ARF-GEF) and inhibits trafficking from endosomes to

the PM, which also prevents recycling of endosomes, leading to cargo accumulation in BFA-induced compartments called BFA bodies (Robinson *et al.*, 2008). In plants co-treated with BFA and cycloheximide (CHX) we found TOL5:VENUS, TOL5:mcherry, and TOL2:VENUS to clearly colocalize with RFP:PYR1, GFP:PYL4 and GFP:ABCG25 in BFA bodies (Figs 6b, S7b, middle panels).

To further characterize endomembrane compartments in which TOLs reside together with their cargo, we perturbed trafficking to the vacuole with Wm. FP-tagged ABA receptors and GFP:ABCG25 showed a distinct accumulation in Wm bodies, indicating that they are trapped in enlarged MVBs en route to the vacuole for degradation. Similarly, TOL2 and TOL5 reporter proteins, localize to distinct endomembrane compartments when trafficking is perturbed by Wm, exhibiting a clear overlap with ABA receptors and ABCG25 reporter signals (Figs 6c, S7b, right panels). Colocalization of FP-tagged TOL5 with PM-residing ABCG25, but also of TOL2 and TOL5 with cargo that shows only limited recruitment to the PM like the PYR1 and PYL4 ABA receptors, is in line with these TOLs functioning in the sorting of these cargos. This argues for a more diversified function of TOLs in sorting processes, not restricted to PM proteins.

Aberrations in stomatal size and opening and higher foliar leaf temperature in *tol2/3/5/6* prompted us to test for expression of the TOLs in guard cells where indeed, VENUS signals of all four TOLs expressed under their endogenous promoter were observed (Fig. 7), indicating that *TOLs* function in this highly specialized cell type. Furthermore, TOL reporter signals colocalized with overexpressed RFP:PYR1 in the cytoplasm and in vesicular structures of guard cells (Fig. 7, white arrows). In an earlier report, promoter-GUS analysis of *PYR1* revealed expression in guard cells (Gonzalez-Guzman *et al.*, 2012). Consistently, expression of *PYR1p::PYR1:GFP*, resulted in signals in guard cells, in cytoplasm, vesicular structures and the nucleus, resembling those observed in *35S::RFP:PYR1* lines (Fig. S8). Thus, apart from co-expression in root meristem cells, co-expression of TOLs with the ABA receptor in guard cells could point at a regulatory role TOLs play in stomatal opening by controlling the abundance of the ABA receptor PYR1.

In summary, colocalization of selected TOL reporter proteins and elements of the ABA signaling/homeostasis machinery is consistent with a scenario, in which TOL adaptor proteins modulate the cellular impact of ABA by adjusting steady-state levels of ABA receptors and transporters.

TOL proteins affect the stability and vacuolar trafficking of ABA receptors and transporters

To attenuate signaling, elevated ABA levels cause downregulation of ABA receptors by promoting their degradation in the vacuole (Belda-Palazon *et al.*, 2016; Yu *et al.*, 2016a; Garcia-Leon *et al.*, 2019). To determine if TOL proteins are involved in the regulation of ABA receptor and transporter abundance, we investigated consequences of loss of *TOL* genes on the stability of PYR1 and PYL4.

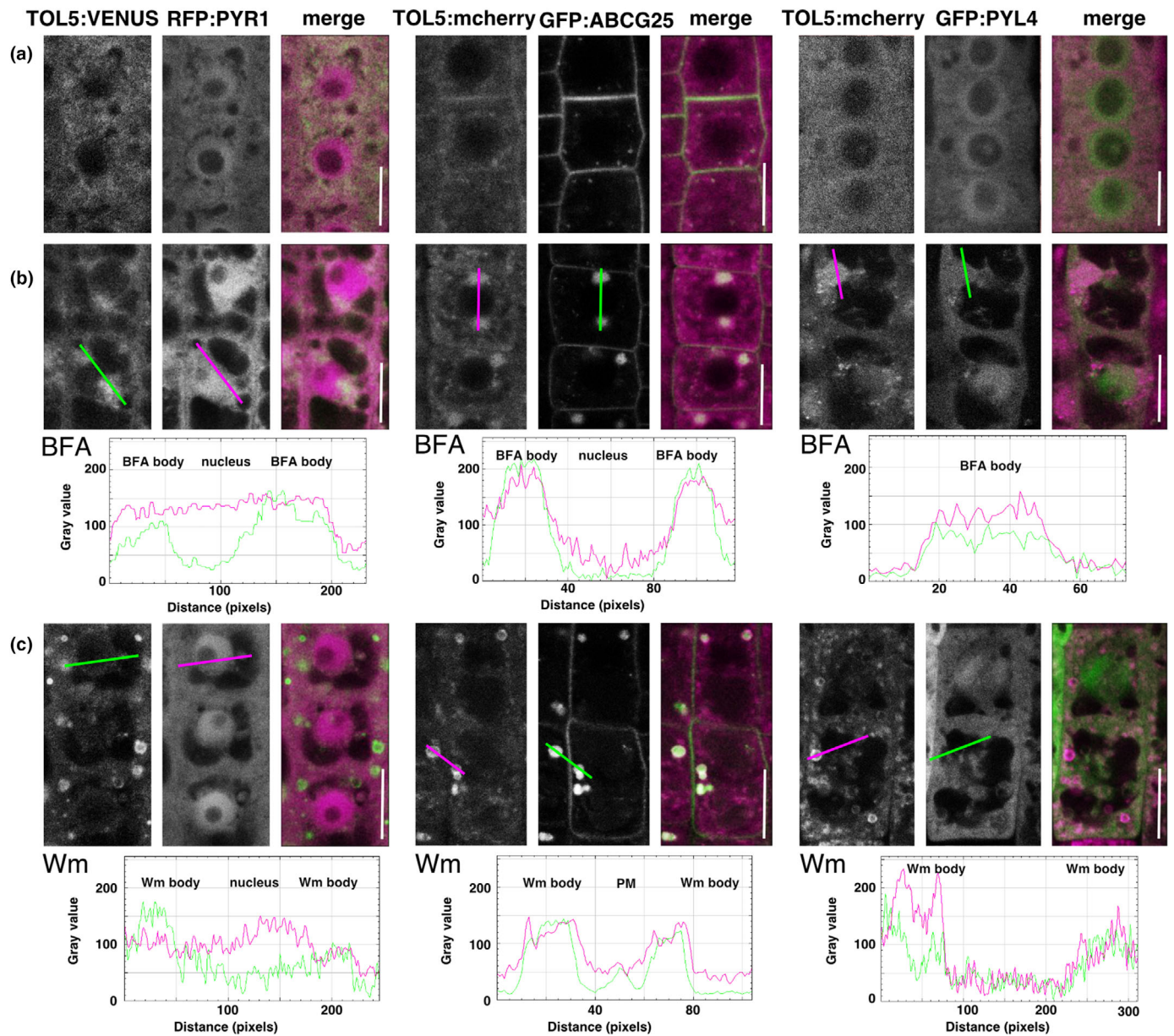


Fig. 6 Colocalization of FP-tagged TOL5 with FP-tagged ABA receptors and transporters in different endosomal compartments. Plant lines co-expressing *TOL5p::TOL5:VENUS/35S::RFP:PYR1* (left panels), *TOL5p::TOL5:mcherry/35S::GFP:ABCG25* (middle panels) or *TOL5p::TOL5:mcherry/35S::GFP:PYL4* (right panels) were either mock-treated (a) or treated with 50 μM BFA and 50 μM CHX (which inhibits *de novo* protein synthesis) (b) or with 33 μM Wm (c). Root epidermis cells of 6 DAG seedlings were analyzed using CLSM. Bars: 10 μm . Profile of RFP (magenta) or VENUS (green) (left panels), mcherry (magenta) or GFP (green) (middle and right panels) signal intensity along a straight line were acquired by IMAGEJ and depicted underneath the corresponding figures. The PM, nucleus, BFA or Wm bodies areas are indicated.

We first employed immunoblot analysis of endogenous PYR1 in total protein extracts of seedlings germinated on control or 0.3 μM ABA-containing medium (Fig. 8a). While protein levels of endogenous PYR1 in WT and *tol2/3/5/6* protein extracts showed no significant difference under control conditions, there was a pronounced difference when seedlings were grown on ABA. Upon ABA treatment, the majority of PYR1 was degraded in WT while it appeared stabilized in *tol2/3/5/6*, with roughly half the protein remaining undegraded (Fig. 8a). Similar results

were obtained with *35S::GFP:PYL4*. No differences in protein levels were observed when comparing WT and isogenic *tol2/3/5/6* expressing *35S::GFP:PYL4* under control conditions. By contrast, when grown on ABA, a stabilization of GFP:PYL4 could be observed in *tol2/3/5/6*, when compared to wild-type (Fig. 8b). In the severe *tolQ* mutant, we detected strong ectopic accumulation of ubiquitinated proteins, reflecting the function of *TOLs* in initiating the degradation of ubiquitinated cargo, which we did not detect in *tol2/3/5/6* (Fig. 1b). Nevertheless, *tol2/3/5/6* exhibits

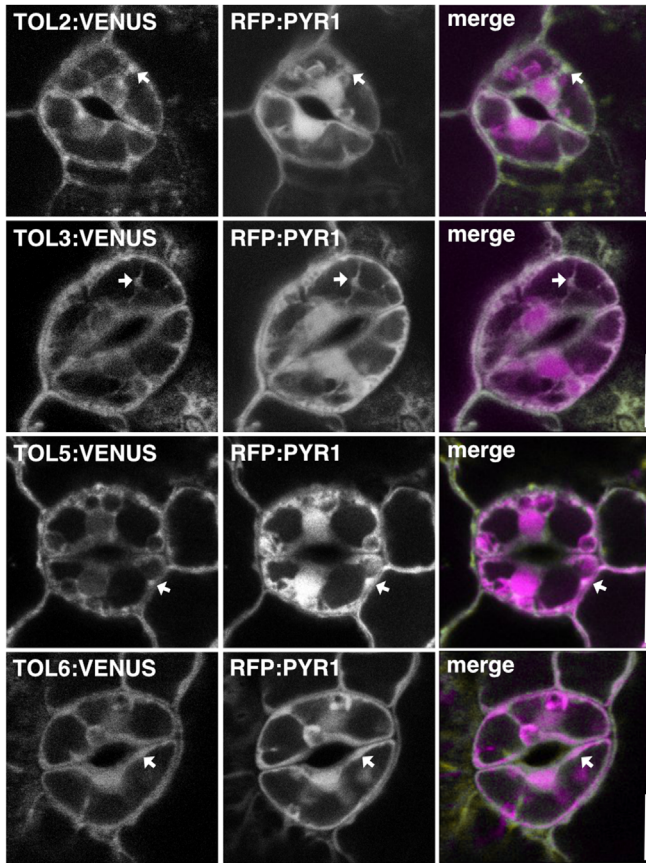


Fig. 7 Colocalization VENUS tagged TOL2,3,5 and 6 with RFP-tagged PYR1 in guard cells of stomata. Cotyledons of 6 DAG seedlings of plant lines co-expressing *TOL2p::TOL2:VENUS*, *TOL3p::TOL3:VENUS*, *TOL5p::TOL5:VENUS* or *TOL6p::TOL6:VENUS* with *35S::RFP:PYR1* were analyzed using CLSM. Arrows indicate colocalization of the two reporter signals. Bars: 10 μ m.

defect in the control of ABA receptor protein homeostasis and thus could specifically lead to enhanced accumulation of ubiquitinated ABA receptors. To test this possibility, we prepared protein extracts from isogenic Col-0 and *tol2/3/5/6* plant lines expressing GFP-tagged PYR1, immunoprecipitated the GFP-tagged protein and tested it for ubiquitination with a ubiquitin-specific antibody (Fig. 8c). This revealed an increase in the ubiquitination of GFP:PYR1 in *tol2/3/5/6* plant extracts when compared to WT controls. The difference was not as obvious in untreated samples, but prominent in the ABA-treated material. This indicates that ubiquitinated GFP:PYR1, whilst efficiently turned over in the WT, accumulates in *tol2/3/5/6*, altogether suggestive of deficiencies in ubiquitinated PYR1 cargo recognition and/or endocytic sorting in the mutant.

Further evidence for TOL proteins modulating the turnover of elements of the ABA signaling/homeostasis machinery comes from analysis of GFP:ABCG25 signals in WT and *tol2/3/5/6*. When treating isogenic lines expressing *35S::GFP:ABCG25* with Wm to assess differences in vacuolar sorting, we detected GFP signals inside well-defined Wm bodies in the WT background, where the membrane dye FM4-64 is found to demarcate these

structures (Fig. 9 upper panels). Conversely, in *tol2/3/5/6*, even though Wm bodies are clearly discernible, these do not accumulate GFP signals. Instead, GFP:ABCG25 signals are found in smaller clusters that do not stain as prominently with the membrane dye (Fig. 9 lower panels), altogether indicative of GFP:ABCG25 mis-sorting in *tol2/3/5/6*.

Together, results obtained in these experiments are consistent with a participation of selected TOL proteins in correct endocytic sorting and turnover of elements of the ABA signaling/transport machinery.

Discussion

Since deregulated responses to hormonal signals result in detrimental effects on plant vitality, plants have evolved diverse mechanisms for attenuating signals once the stress dissipates. Regulated protein turnover, in which both 26S proteasome and vacuolar degradation pathways are involved, represent a major mechanism for ABA desensitization and termination of the signaling cascade (Yu *et al.*, 2016b; Yu & Xie, 2017). Interestingly, some PYL/PYR/RCAR receptors, even though they are mainly found in the cytosol and nucleus, undergo vacuolar degradation via the ESCRT machinery. All three reported ESCRT subunits, *VPS23A*, *FYVE1/FREE1* and *ALIX*, responsible for targeting the ABA receptors for vacuolar degradation, directly interact with them, indicating a very specific mode of action (Belda-Palazon *et al.*, 2016; Yu *et al.*, 2016a; Garcia-Leon *et al.*, 2019). TOLs are ubiquitin receptors, which bring ubiquitinated cargo destined for degradation to the ESCRT machinery, functioning as ESCRT-0 substitutes (Moulinier-Anzola *et al.*, 2020). In this report we show that discrete TOL proteins attenuate ABA signaling and provide evidence for their requirement in the homeostatic control of protein distribution/levels upon ABA treatment, establishing a function of the TOLs not only in control of ABA receptors but also of transporters via endosomal trafficking.

We could link specific *TOL* genes, *TOL2,3,5* and *6*, to the adjustment of ABA responses in *Arabidopsis*. *Tol2/3/5/6* shows no obvious developmental phenotypes, does not display an extensive accumulation of ubiquitinated cargo and has a normal vacuolar morphology, thereby differing from phenotypes described for a number of ESCRT mutants (Gao *et al.*, 2014; Kalinowska *et al.*, 2015; Kolb *et al.*, 2015; Nagel *et al.*, 2017; Moulinier-Anzola *et al.*, 2020). Nevertheless, *tol2/3/5/6* shows clear drought tolerance accompanied by strong ABA hypersensitivity. All four *TOL* genes are upregulated upon ABA treatment and additively involved in ABA responses, as all possible triple mutant combinations showed weaker responses than *tol2/3/5/6*.

TOLs function in initiating degradative vacuolar sorting of PYR1, PYL4 and ABCG25, as their FP-tagged constructs colocalize with FP-tagged TOL5 and TOL2 in different endosomal compartments of the degradation pathway to the vacuole. Furthermore, endogenous PYR1 and GFP-PYL4 are both stabilized upon ABA treatment in *tol2/3/5/6*, indicating that TOL proteins are indeed required for their degradation. Additionally, ubiquitinated ABA receptors accumulate in *tol2/3/5/6*, specifically upon ABA treatment.

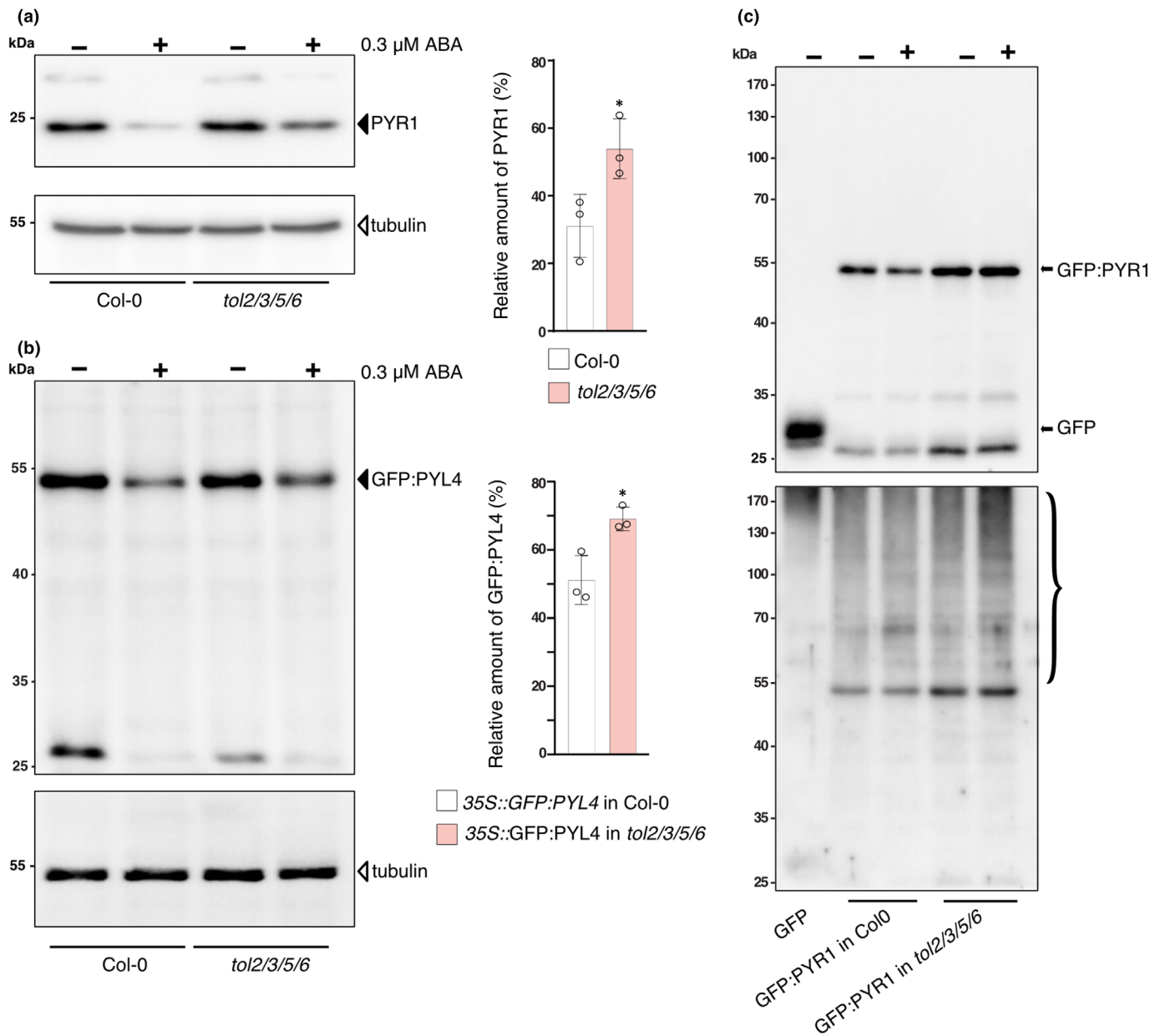


Fig. 8 *tol2/3/5/6* show stabilization of ubiquitinated ABA receptors. Immunoblot showing stabilization of endogenous PYR1 (a) and GFP:PYL4 (b) in *tol2/3/5/6* compared to wild-type (WT) seedlings when grown presence or absence of 0.3 μM ABA. Total protein extracts of 8 DAG *tol2/3/5/6* or Col-0 seedlings (a) or 35S::GFP:PYL4 in *tol2/3/5/6* or Col-0 roots (b) were extracted and subjected to SDS-PAGE and immunoblotting using an anti-PYR1 antibody (a) or anti-GFP antibody (b) (upper panels) or anti-tubulin antibody (lower panel) as a loading control for normalization. Full arrowheads indicate endogenous PYR1 (a) or GFP-PYL4 (b) while the tubulin is represented by the open arrowhead. Band intensities were quantified using IMAGEJ. PYR1 (a) or GFP:PYL4 (b) protein bands were normalized to their corresponding tubulin bands. The graphs on the right represent mean values ± SD of the relative amount of protein (normalized amount of protein with ABA treatment/normalized amount of mock-treated protein) that are stabilized after ABA treatment for each plant line from three independent experiments (student's *t*-test) of PYR1 (*, $P = 0.03697$) (a) and GFP:PYL4 (*, $P = 0.01764$). (b) For both endogenous PYR1 as well as GFP:PYL4 a clear stabilization after ABA treatment can be observed in the *tol2/3/5/6* line when compared to WT. (c) Increased ubiquitination of GFP:PYR1 upon ABA treatment in *tol2/3/5/6* background compared to Col-0. 7 DAG seedlings expressing GFP (as a control) or GFP:PYR1 either in Col-0 or in *tol2/3/5/6* background were sprayed with 100 μM ABA or just solvent as control and harvested after 4 h, GFP-TRAP® agarose beads were used to precipitate GFP or GFP:PYR1 from lysates. Proteins were eluted, separated by SDS-PAGE and analyzed by immunoblotting with anti-GFP (upper panel) and anti-Ubq (P4D1; lower panel) antibodies. Western blots showing input are depicted in Supporting Information Fig. S9.

When testing genetic crosstalk between TOL genes and additional loci participating in ABA responses, there were no apparent synergies with the ABA biosynthesis pathway, while synergies

with the signaling pathway are eminent. The slightly enhanced ABA sensitivity observable in the hextuple *hab1-1abi-2 tol2/3/5/6* compared to its parental lines, is similar to that

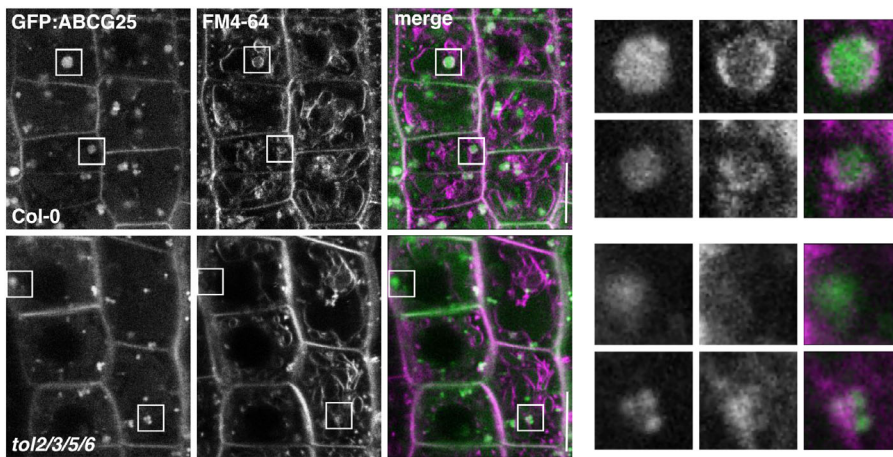


Fig. 9 *tol2/3/5/6* shows altered trafficking for degradation of ABA transporters. 35S::GFP::ABCG25 expressing wild-type (Col-0) (upper panels) or *tol2/3/5/6* (lower panels) seedlings were stained with FM4-64 and then treated with 33 μ M Wm. Root epidermis cells of 6 DAG seedlings were analyzed using CLSM. The small panels next to the respective panel show enlarged (4 \times) views of the boxed regions. Bars: 10 μ m.

described for *vps23a* with *hab1-1abi1-2* (Yu *et al.*, 2016a). Such additivity specifically in responses to ABA, implies nonoverlapping effects of PP2Cs and TOLs in mediating ABA responses. Deficiencies in the sorting of ABA transporters ABCG25 in *tol2/3/5/6* are consistent with such nonoverlapping effects. Additionally, there are other clade-A PP2Cs next to *HAB1* and *ABI1* (Schweighofer *et al.*, 2004), which could likewise be affected by loss of the four *TOLs*.

While interaction between VPS23A and TOLs (Moulinier-Anzola *et al.*, 2020) and VPS23A and FYVE1/FREE1 (Gao *et al.*, 2014) have been shown, no direct interaction between FREE1/FYVE1 and TOLs has been shown to date. Nevertheless, this was only assessed for TOL4 and 9 (Belda-Palazon *et al.*, 2016), which so far have not been linked to attenuating ABA signaling. Thus, future studies could help unravel if specific degradation hubs could form upon ABA signaling.

Loss of *TOL2,3,5* and *6* masks the phenotype of *vps23a* in control of ABA responses, implying that TOLs function upstream of ESCRT-I subunits but results in no obvious growth or developmental phenotype. Nevertheless, further removal of *VPS23A* yields a mild retardation in growth and development. Since five TOLs, namely *TOL2,3,5,6* and *9*, are needed to fully substitute for the ESCRT-0 complex (Korbei *et al.*, 2013), this signifies that *TOL2,3,5* and *6* alone are not completely epistatic to *VPS23A* in development, contrary to their function in ABA signaling. Furthermore, although we did not observe general ectopic accumulation of ubiquitinated cargo (as in the *tolQ*) in the *tol2/3/5/6* plant line, ABA treatment results in a disproportional accumulation of ubiquitinated ABA receptor cargo in *tol2/3/5/6*. These findings link the function of a distinct group of *TOL* genes to the regulation of ABA signaling.

Whilst alterations in the stability of ABA receptors will evidently affect ABA signal transmission, the apparent mislocalization of ABCG25 in *tol2/3/5/6* late endosomes/MVBs could also contribute to altered ABA responsiveness. ABA transporters can function as importers or exporters and their spatial distribution is key to their function. Thus, how alterations in their degradation affects ABA signaling is difficult to predict (Zhang *et al.*, 2023). ABCG25 activity is involved in the control of seed

germination and dormancy, where ABCG25 and ABCG31 jointly transport ABA out of the endosperm (Kang *et al.*, 2015). Alterations in ABA homeostasis caused by ABCG25 stabilization thus could contribute to the phenotypes observed in *tol2/3/5/6*.

Expression patterns and functional analysis of ABA transporters in guard cells indicate that they are required for the modulation of ABA signals, where ABCG25 delivers ABA to guard cells and thereby impacts on stomatal closure (Kang *et al.*, 2010; Kurumori *et al.*, 2010). ABA receptors localize to guard cells as well (Gonzalez-Guzman *et al.*, 2012). The apparent colocalization of RFP-tagged PYR1 and TOL proteins in stomata guard cells could point to an involvement of ESCRT-mediated vacuolar targeting of ABA receptors in these highly specialized cells. Support for this comes from observations in which ALIX was found to localize in the cytosol and vesicle-like compartments of guard cells (Garcia-Leon *et al.*, 2019), a localization similar to TOL: Venus reporter proteins and RFP:PYR1. Thus, aberrations in stomatal aperture that we observed in *tol2/3/5/6* could point towards a role for ESCRT machinery in guard cells where in particular TOLs regulate the function of ABA receptors and ABA transporters, ensuring correct and timely stomata opening and closing.

ABA signaling pathways are a potential target to improve plant performance under drought, where mutants showing enhanced ABA responses, lead to more stress-tolerant phenotypes. Degradation of components of the ABA signaling machinery is an important factor to modulate the attenuation of the hormonal signaling and several components of the ESCRT machinery have been shown to play very active roles in this process (Belda-Palazon *et al.*, 2016; Yu *et al.*, 2016a; Garcia-Leon *et al.*, 2019). Nevertheless, the partial loss-of-function plant line *alix-1* shows strong developmental defects with morphological alterations in the vacuoles in general and of the guard cells in particular (Cardona-Lopez *et al.*, 2015; Garcia-Leon *et al.*, 2019). Similarly, different *fve1* mutant alleles as well as the total loss-of-function mutant *vps23a* showed strong alterations in the nuclear morphology (Belda-Palazon *et al.*, 2016; Yu *et al.*, 2016a; Lou *et al.*, 2020) making them difficult targets for engineering drought tolerance. Furthermore, *alix-1* and *fve1* mutant plant lines show constitutive ABA response and differences in their endogenous

ABA levels under standard growth conditions (Belda-Palazon *et al.*, 2016; Garcia-Leon *et al.*, 2019). In *tol2/3/5/6* we observed no negative impact on plant growth and development, and no alterations in vacuolar morphology. Furthermore, endogenous ABA content or constitutive ABA response were unaffected. Subtler effects could be achieved through mutating not all four but potentially only one or two of the *TOLs*, thus making them ideal candidates to improve plant performance under drought stress. Trying to decipher which determinants in the *TOLs* are essential for their role in ABA signaling pathway will be an interesting scope for future studies.

Acknowledgements

We would like to thank Vicente Rubio for providing *hab1-1abi1-2* and *pyr1pyl4pyl5pyl8* seeds. We thank the Plant Hormone Quantification Service, IBMCP, Valencia, Spain who carried out the hormone quantification and the BOKU-VIBT Imaging Center and M. Debreczeny for access and advice. This work was supported by the Austrian Science Fund (FWF) [grant nos. FWF P34748, P30850, P33989 to BK, V690-B25 to EF and P31493 to CL] and by the Gesellschaft für Forschungsförderung Niederösterreich m.b.H.: FTI19-008 to CL. Work at JL-J group is funded by MICIN/AEI with PID2021-128826OA-I00 and RYC2020-029097-I, Plan GenT (CISEJI/2022/26) from Generalitat Valenciana (GVA) grants and the AGROALNEXT/2022/067 grant supported by MICIN with funding from European Union NextGenerationEU (PRTR-C17.I1) and by Generalitat Valenciana.






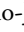
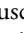
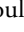

Competing interests

None declared.

Author contributions

BK conceived and supervised this study. Methodology, JM-A, MS, EF, JL-J and BK; Investigation, JM-A, MS, RL, MIF, NL, IT, EA, EF, JL-J and BK; Writing – Original Draft, BK and JM-A; Writing – Review & Editing, CL and BK; Funding Acquisition, CL, JL-J, EF and BK. All authors approved the submission of the final draft.

ORCID

Elsa Arcalis  <https://orcid.org/0000-0001-9883-465X>
 Elena Feraru  <https://orcid.org/0000-0003-1979-2661>
 Mugurel I. Feraru  <https://orcid.org/0000-0002-3484-1110>
 Barbara Korbei  <https://orcid.org/0000-0002-0439-0435>
 Nils Leibrock  <https://orcid.org/0000-0002-5350-9260>
 Jorge Lozano-Juste  <https://orcid.org/0000-0001-7034-566X>
 Christian Mouschnig  <https://orcid.org/0000-0003-2099-9280>
 Jeanette Moulinier-Anzola  <https://orcid.org/0000-0001-8635-7227>
 Maximilian Schwihla  <https://orcid.org/0000-0001-6887-5661>

Data availability

All data supporting the findings of this study are available within the paper and in the [Supporting Information](#) of this article. Materials of this study are available from the corresponding author.

References

- Ali A, Pardo JM, Yun DJ. 2020. Desensitization of ABA-signaling: the swing from activation to degradation. *Frontiers in Plant Science* 11: 379.
- Alqurashi M, Chiapello M, Bianchet C, Paolucci F, Lilley KS, Gehring C. 2018. Early responses to severe drought stress in the *Arabidopsis thaliana* cell suspension culture proteome. *Proteomes* 6: 38.
- Barrera JM, Piqueras P, Gonzalez-Guzman M, Serrano R, Rodriguez PL, Ponce MR, Micol JL. 2005. A mutational analysis of the ABA1 gene of *Arabidopsis thaliana* highlights the involvement of ABA in vegetative development. *Journal of Experimental Botany* 56: 2071–2083.
- Belda-Palazon B, Rodriguez L, Fernandez MA, Castillo MC, Anderson EA, Gao C, Gonzalez-Guzman M, Peirats-Llobet M, Zhao Q, De Winne N *et al.* 2016. FYVE1/FREE1 interacts with the PYL4 ABA receptor and mediates its delivery to the vacuolar degradation pathway. *Plant Cell* 28: 2291–2311.
- Bilodeau PS, Winistorfer SC, Kearney WR, Robertson AD, Piper RC. 2003. Vps27-Hse1 and ESCRT-I complexes cooperate to increase efficiency of sorting ubiquitinated proteins at the endosome. *The Journal of Cell Biology* 163: 237–243.
- Bueso E, Rodriguez L, Lorenzo-Orts L, Gonzalez-Guzman M, Sayas E, Munoz-Bertomeu J, Ibanez C, Serrano R, Rodriguez PL. 2014. The single-subunit RING-type E3 ubiquitin ligase RSL1 targets PYL4 and PYR1 ABA receptors in plasma membrane to modulate abscisic acid signaling. *The Plant Journal* 80: 1057–1071.
- Cardona-Lopez X, Cuyas L, Marin E, Rajulu C, Irigoyen ML, Gil E, Puga MI, Bligny R, Nussaume L, Geldner N *et al.* 2015. ESCRT-III-associated protein ALIX mediates high-affinity phosphate transporter trafficking to maintain phosphate homeostasis in *Arabidopsis*. *Plant Cell* 27: 2560–2581.
- Chen L, Hellmann H. 2013. Plant E3 ligases: flexible enzymes in a sessile world. *Molecular Plant* 6: 1388–1404.
- Clough SJ, Bent AF. 1998. Floral dip: a simplified method for *Agrobacterium*-mediated transformation of *Arabidopsis thaliana*. *The Plant Journal* 16: 735–743.
- Cutler SR, Rodriguez PL, Finkelstein RR, Abrams SR. 2010. Abscisic acid: emergence of a core signaling network. *Annual Review of Plant Biology* 61: 651–679.
- Diaz M, Sanchez-Barrena MJ, Gonzalez-Rubio JM, Rodriguez L, Fernandez D, Antoni R, Yunta C, Belda-Palazon B, Gonzalez-Guzman M, Peirats-Llobet M *et al.* 2016. Calcium-dependent oligomerization of CAR proteins at cell membrane modulates ABA signaling. *Proceedings of the National Academy of Sciences, USA* 113: E396–E405.
- Fernandez MA, Belda-Palazon B, Julian J, Coego A, Lozano-Juste J, Inigo S, Rodriguez L, Bueso E, Goossens A, Rodriguez PL. 2020. RBR-type E3 ligases and the ubiquitin-conjugating enzyme UBC26 regulate abscisic acid receptor levels and signaling. *Plant Physiology* 182: 1723–1742.
- Finkelstein R. 2013. Abscisic acid synthesis and response. *The Arabidopsis Book* 11: e0166.
- Gao C, Luo M, Zhao Q, Yang R, Cui Y, Zeng Y, Xia J, Jiang L. 2014. A unique plant ESCRT component, FREE1, regulates multivesicular body protein sorting and plant growth. *Current Biology* 24: 2556–2563.
- Garcia-Leon M, Cuyas L, El-Moneim DA, Rodriguez L, Belda-Palazon B, Sanchez-Quant E, Fernandez Y, Roux B, Zamarreno AM, Garcia-Mina JM *et al.* 2019. *Arabidopsis* ALIX regulates stomatal aperture and turnover of abscisic acid receptors. *Plant Cell* 31: 2411–2429.
- Gonzalez Solis A, Berryman E, Otegui MS. 2022. Plant endosomes as protein sorting hubs. *FEBS Letters* 596: 2288–2304.
- Gonzalez-Guzman M, Pizzio GA, Antoni R, Vera-Sirera F, Merilo E, Bassel GW, Fernández MA, Holdsworth MJ, Perez-Amador MA, Kollist H *et al.*

2012. Arabidopsis PYR/PYL/RCAR receptors play a major role in quantitative regulation of stomatal aperture and transcriptional response to abscisic acid. *Plant Cell* 24: 2483–2496.
- Isono E. 2020. TOL keepers for ubiquitin-mediated trafficking routes in plant cells. *Molecular Plant* 13: 685–687.
- Isono E, Kalinowska K. 2017. ESCRT-dependent degradation of ubiquitylated plasma membrane proteins in plants. *Current Opinion in Plant Biology* 40: 49–55.
- Kalinowska K, Nagel MK, Goodman K, Cuyas L, Anzenberger F, Alkofer A, Paz-Ares J, Braun P, Rubio V, Otegui MS *et al.* 2015. Arabidopsis ALIX is required for the endosomal localization of the deubiquitinating enzyme AMSH3. *Proceedings of the National Academy of Sciences, USA* 112: E5543–E5551.
- Kang J, Hwang JU, Lee M, Kim YY, Assmann SM, Martinoia E, Lee Y. 2010. PDR-type ABC transporter mediates cellular uptake of the phytohormone abscisic acid. *Proceedings of the National Academy of Sciences, USA* 107: 2355–2360.
- Kang J, Yim S, Choi H, Kim A, Lee KP, Lopez-Molina L, Martinoia E, Lee Y. 2015. Abscisic acid transporters cooperate to control seed germination. *Nature Communications* 6: 8113.
- Kolb C, Nagel MK, Kalinowska K, Haggmann J, Ichikawa M, Anzenberger F, Alkofer A, Sato MH, Braun P, Isono E. 2015. FYVE1 is essential for vacuole biogenesis and intracellular trafficking in Arabidopsis. *Plant Physiology* 167: 1361–1373.
- Korbei B, Moulinier-Anzola J, De-Araujo L, Lucyshyn D, Retzer K, Khan MA, Luschign C. 2013. Arabidopsis TOL proteins act as gatekeepers for vacuolar sorting of PIN2 plasma membrane protein. *Current Biology* 23: 2500–2505.
- Kuromori T, Miyaji T, Yabuuchi H, Shimizu H, Sugimoto E, Kamiya A, Moriyama Y, Shinozaki K. 2010. ABC transporter AtABCG25 is involved in abscisic acid transport and responses. *Proceedings of the National Academy of Sciences, USA* 107: 2361–2366.
- Leon-Kloosterziel KM, Gil MA, Ruijs GJ, Jacobsen SE, Olszewski NE, Schwartz SH, Zeevaert JA, Koornneef M. 1996. Isolation and characterization of abscisic acid-deficient Arabidopsis mutants at two new loci. *The Plant Journal* 10: 655–661.
- Liang C, Li C, Wu J, Zhao M, Chen D, Liu C, Chu J, Zhang W, Hwang J, Wang M. 2022. SORTING NEXIN2 proteins mediate stomatal movement and the response to drought stress by modulating trafficking and protein levels of the ABA exporter ABCG25. *The Plant Journal* 110: 1603–1618.
- Lou L, Yu F, Tian M, Liu G, Wu Y, Wu Y, Xia R, Pardo JM, Guo Y, Xie Q. 2020. ESCRT-I component VPS23A sustains salt tolerance by strengthening the SOS module in Arabidopsis. *Molecular Plant* 13: 1134–1148.
- Ma Y, Szostkiewicz I, Korte A, Moes D, Yang Y, Christmann A, Grill E. 2009. Regulators of PP2C phosphatase activity function as abscisic acid sensors. *Science* 324: 1064–1068.
- Merlot S, Leonhardt N, Fenzi F, Valon C, Costa M, Piette L, Vavasseur A, Genty B, Boivin K, Muller A *et al.* 2007. Constitutive activation of a plasma membrane H(+)-ATPase prevents abscisic acid-mediated stomatal closure. *EMBO Journal* 26: 3216–3226.
- Merlot S, Mustilli AC, Genty B, North H, Lefebvre V, Sotta B, Vavasseur A, Giraudat J. 2002. Use of infrared thermal imaging to isolate Arabidopsis mutants defective in stomatal regulation. *The Plant Journal* 30: 601–609.
- Moulinier-Anzola J, De-Araujo L, Korbei B. 2014. Expression of Arabidopsis TOL genes. *Plant Signaling & Behavior* 9: e28667.
- Moulinier-Anzola J, Schwihla M, De-Araujo L, Artner C, Jörg L, Konstantinova N, Luschign C, Korbei B. 2020. TOLs function as ubiquitin receptors in the early steps of the ESCRT pathway in higher plants. *Molecular Plant* 13: 717–731.
- Munemasa S, Hauser F, Park J, Waadt R, Brandt B, Schroeder JI. 2015. Mechanisms of abscisic acid-mediated control of stomatal aperture. *Current Opinion in Plant Biology* 28: 154–162.
- Murashige T, Skoog F. 1962. A revised medium for rapid growth and bio assays with tobacco tissue cultures. *Physiologia Plantarum* 15: 473–497.
- Nagel MK, Kalinowska K, Vogel K, Reynolds GD, Wu Z, Anzenberger F, Ichikawa M, Tsutsumi C, Sato MH, Kuster B *et al.* 2017. Arabidopsis SH3P2 is an ubiquitin-binding protein that functions together with ESCRT-I and the deubiquitylating enzyme AMSH3. *Proceedings of the National Academy of Sciences, USA* 114: E7197–E7204.
- Nakashima K, Fujita Y, Katsura K, Maruyama K, Narusaka Y, Seki M, Shinozaki K, Yamaguchi-Shinozaki K. 2006. Transcriptional regulation of ABI3- and ABA-responsive genes including RD29B and RD29A in seeds, germinating embryos, and seedlings of Arabidopsis. *Plant Molecular Biology* 60: 51–68.
- Nakashima K, Yamaguchi-Shinozaki K. 2013. ABA signaling in stress-response and seed development. *Plant Cell Reports* 32: 959–970.
- Nguyen HH, Lee MH, Song K, Ahn G, Lee J, Hwang I. 2018. The A/ENTH domain-containing protein AtECA4 is an adaptor protein involved in cargo recycling from the trans-golgi network/early endosome to the plasma membrane. *Molecular Plant* 11: 568–583.
- Park SY, Fung P, Nishimura N, Jensen DR, Fujii H, Zhao Y, Lumba S, Santiago J, Rodrigues A, Chow TF *et al.* 2009. Abscisic acid inhibits type 2C protein phosphatases via the PYR/PYL family of START proteins. *Science* 324: 1068–1071.
- Park Y, Xu ZY, Kim SY, Lee J, Choi B, Lee J, Kim H, Sim HJ, Hwang I. 2016. Spatial regulation of ABCG25, an ABA exporter, is an important component of the mechanism controlling cellular ABA levels. *Plant Cell* 28: 2528–2544.
- Robinson DG, Jiang L, Schumacher K. 2008. The endosomal system of plants: charting new and familiar territories. *Plant Physiology* 147: 1482–1492.
- Rodríguez L, Gonzalez-Guzman M, Diaz M, Rodrigues A, Izquierdo-Garcia AC, Peirats-Llobet M, Fernandez MA, Antoni R, Fernandez D, Marquez JA *et al.* 2014. C2-domain abscisic acid-related proteins mediate the interaction of PYR/PYL/RCAR abscisic acid receptors with the plasma membrane and regulate abscisic acid sensitivity in Arabidopsis. *Plant Cell* 26: 4802–4820.
- Saez A, Robert N, Maktabi MH, Schroeder JI, Serrano R, Rodriguez PL. 2006. Enhancement of abscisic acid sensitivity and reduction of water consumption in Arabidopsis by combined inactivation of the protein phosphatases type 2C ABI1 and HAB1. *Plant Physiology* 141: 1389–1399.
- Schweighofer A, Hirt H, Meskiene I. 2004. Plant PP2C phosphatases: emerging functions in stress signaling. *Trends in Plant Science* 9: 236–243.
- Schwihla M, Korbei B. 2020. The beginning of the end: initial steps in the degradation of plasma membrane proteins. *Frontiers in Plant Science* 11: 680.
- Shu K, Liu XD, Xie Q, He ZH. 2016. Two faces of one seed: hormonal regulation of dormancy and germination. *Molecular Plant* 9: 34–45.
- Shu K, Yang W. 2017. E3 ubiquitin ligases: ubiquitous actors in plant development and abiotic stress responses. *Plant & Cell Physiology* 58: 1461–1476.
- Weiner JJ, Peterson FC, Volkman BF, Cutler SR. 2010. Structural and functional insights into core ABA signaling. *Current Opinion in Plant Biology* 13: 495–502.
- Yu F, Lou L, Tian M, Li Q, Ding Y, Cao X, Wu Y, Belda-Palazon B, Rodriguez PL, Yang S *et al.* 2016a. ESCRT-I component VPS23A affects ABA signaling by recognizing ABA receptors for endosomal degradation. *Molecular Plant* 9: 1570–1582.
- Yu F, Wu Y, Xie Q. 2016b. Ubiquitin-proteasome system in ABA signaling: from perception to action. *Molecular Plant* 9: 21–33.
- Yu F, Xie Q. 2017. Non-26S proteasome endomembrane trafficking pathways in ABA signaling. *Trends in Plant Science* 22: 976–985.
- Zhang Y, Berman A, Shani E. 2023. Plant hormone transport and localization: signaling molecules on the move. *Annual Review of Plant Biology* 74: 453–479.
- Zhao H, Nie K, Zhou H, Yan X, Zhan Q, Zheng Y, Song CP. 2020. ABI5 modulates seed germination via feedback regulation of the expression of the PYR/PYL/RCAR ABA receptor genes. *New Phytologist* 228: 596–608.

Supporting Information

Additional Supporting Information may be found online in the Supporting Information section at the end of the article.

Fig. S1 Wilting phenotype of and guard cell size in *tol2/3/5/6*.

Fig. S2 Expression analysis and additive phenotype in ABA response of *TOL2,3,5* and *6*.

Fig. S3 Phenotypes of flowering plants lines.

Fig. S4 Colocalization of the membrane dye FM4-64 with ABA receptors and transporters in endosomal structures.

Fig. S5 *35S::GFP:PYR1* rescues the hyposensitive germination phenotype of *pyr1pyl4pyl5pyl8*.

Fig. S6 *TOL5p::TOL5:VENUS* partially rescues the hypersensitive germination phenotype of *tol2/3/5/6*.

Fig. S7 Localization of TOL3:VENUS, TOL6:VENUS and TOL2:VENUS with RFP:PYR1.

Fig. S8 *35S::GFP:PYR* and *PYR1p::PYR1:GFP* expressing plant lines show the same localization of GFP-tagged PYR1 in guard cells of stomata.

Fig. S9 Input controls for experiment in Fig. 8c.

Table S1 Primers used in this study.

Table S2 Plant lines used in this study.

Table S3 Drugs and stains used for CLSM.

Table S4 Antibodies used in this study.

Please note: Wiley is not responsible for the content or functionality of any Supporting Information supplied by the authors. Any queries (other than missing material) should be directed to the *New Phytologist* Central Office.